

## Port Accessibility Depends on Cascading Interactions between Fleets, Policies, Infrastructure, and Hydrodynamics

Bakker, Floor P.; van der Werff, Solange; Baart, Fedor; Kirichek, Alex ; De Jong, Sander; van Koningsveld, Mark

**DOI**

[10.3390/jmse12061006](https://doi.org/10.3390/jmse12061006)

**Publication date**

2024

**Document Version**

Final published version

**Published in**

Journal of Marine Science and Engineering

**Citation (APA)**

Bakker, F. P., van der Werff, S., Baart, F., Kirichek, A., De Jong, S., & van Koningsveld, M. (2024). Port Accessibility Depends on Cascading Interactions between Fleets, Policies, Infrastructure, and Hydrodynamics. *Journal of Marine Science and Engineering*, 12(6), Article 1006. <https://doi.org/10.3390/jmse12061006>

**Important note**

To cite this publication, please use the final published version (if applicable). Please check the document version above.

**Copyright**

Other than for strictly personal use, it is not permitted to download, forward or distribute the text or part of it, without the consent of the author(s) and/or copyright holder(s), unless the work is under an open content license such as Creative Commons.

**Takedown policy**

Please contact us and provide details if you believe this document breaches copyrights. We will remove access to the work immediately and investigate your claim.

Article

# Port Accessibility Depends on Cascading Interactions between Fleets, Policies, Infrastructure, and Hydrodynamics

Floor P. Bakker <sup>1,\*</sup> , Solange van der Werff <sup>1</sup> , Fedor Baart <sup>1,2</sup> , Alex Kirichek <sup>1</sup> , Sander de Jong <sup>1</sup>   
and Mark van Koningsveld <sup>1,3</sup> 

<sup>1</sup> Faculty of Civil Engineering and Geosciences, Delft University of Technology, Stevinweg 1, P.O. Box 5048, 2628 CN Delft, The Netherlands; s.e.vanderwerff@tudelft.nl (S.v.d.W.); fedor.baart@deltares.nl (F.B.); o.kirichek@tudelft.nl (A.K.); sander\_de\_jong1993@hotmail.com (S.d.J.); m.vankoningsveld@tudelft.nl (M.v.K.)

<sup>2</sup> Deltares, Boussinesqweg 1, P.O. Box 177, 2629 HV Delft, The Netherlands

<sup>3</sup> Van Oord Dredging and Marine Contractors B.V., Schaardijk 211, P.O. Box 8574, 3063 NH Rotterdam, The Netherlands

\* Correspondence: f.p.bakker@tudelft.nl

**Abstract:** Reducing waiting times is crucial for ports to be efficient and competitive. Important causes of waiting times are cascading interactions between realistic hydrodynamics, accessibility policies, vessel-priority rules, and detailed berth availability. The main challenges are determining the cause of waiting and finding rational solutions to reduce waiting time. In this study, we focus on the role of the design depth of a channel on the waiting times. We quantify the performance of channel depth for a representative fleet rather than the common approach of a single normative design vessel. The study relies on a mesoscale agent-based discrete-event model that can take processed Automatic Identification System and hydrodynamic data as its main input. The presented method's validity is assessed by hindcasting one year of observed anchorage area laytimes for a liquid bulk terminal in the Port of Rotterdam. The hindcast demonstrates that the method predicts the causes of 73.4% of the non-excessive laytimes of vessels, thereby correctly modelling 60.7% of the vessels-of-call. Following a recent deepening of the access channel, cascading waiting times due to tidal restrictions were found to be limited. Nonetheless, the importance of our approach is demonstrated by testing alternative maintained bed level designs, revealing the method's potential to support rational decision-making in coastal zones.

**Keywords:** port performance; Automatic Identification System data; mesoscopic traffic model; tidal windows; representative fleet



**Citation:** Bakker, F.P.; van der Werff, S.; Baart, F.; Kirichek, A.; de Jong, S.; van Koningsveld, M. Port Accessibility Depends on Cascading Interactions between Fleets, Policies, Infrastructure, and Hydrodynamics. *J. Mar. Sci. Eng.* **2024**, *12*, 1006. <https://doi.org/10.3390/jmse12061006>

Academic Editors: Václav Pištěk, Xiaoyuan Wang and Longjin Wang

Received: 13 May 2024

Revised: 7 June 2024

Accepted: 11 June 2024

Published: 17 June 2024



**Copyright:** © 2024 by the authors. Licensee MDPI, Basel, Switzerland. This article is an open access article distributed under the terms and conditions of the Creative Commons Attribution (CC BY) license (<https://creativecommons.org/licenses/by/4.0/>).

## 1. Introduction

Access channels and waterways form the gateway to seaports and simultaneously an important element of coasts and estuaries [1]. An 'accessible' port assures the safe and efficient transit of the calling (sea-going) vessels through the channel. Downtime of the access channel can cause significant waiting times for vessels, which decreases the port's efficiency. Tide-related accessibility restrictions are a common cause of downtime, especially for the largest vessels, and therefore considered important for port authorities from a nautical-logistical perspective. A port can moreover be congested, meaning that the capacity of its infrastructure is overloaded. Port congestion and downtime are interconnected, which can lead to cascading effects that increase waiting times and thereby further decrease the port's efficiency [2].

So far, such cascading effects have rarely been considered in port design, as common guidelines typically focus on (the largest) design vessels only [3]. The most common approach to quantify port accessibility is the method described in the Harbour Approach Channels Design Guideline [4]. It quantifies accessibility as the percentage of accessible

tides for the deepest-draughted vessel(s) in the calling fleet (see also [5,6]). Although realistic hydrodynamics and detailed accessibility policies form the basis of this method, it ignores nautical traffic and, consequently, waiting times due to congestion and cascading effects.

Beyond the approach suggested by PIANC [4], various simulation approaches are available that do resolve waiting times, at varying scales, ranging from micro- to macroscopic approaches [7]. Most models in the literature are microscopic, meaning they resolve detailed manoeuvres including vessel–vessel and vessel–infrastructure interactions. They tend to focus on waiting times caused by single components of the port network/infrastructure. Examples include heuristic algorithms that minimize congestion-related waiting times at various types of terminals (i.e., [8–10]), and on the waterway (i.e., [11,12]). Furthermore, analytical agent-based models are available that describe vessel motions and behaviour in waterways (i.e., [13–17]), and discrete-event models that focus on land-based terminal operations (i.e., [18–22]).

Although successful in estimating the delays of individual vessels at specific components of the port, microscopic models are typically unable to cover the entire port network or the full extent of the traffic, due to computational constraints. Furthermore, they rarely include (realistic) hydrodynamics, detailed accessibility policies, specific berth layouts, and berth-allocation policies.

In contrast to the amount of microscopic models, only a few macroscopic shipping models are discussed in the literature. These models focus on traffic flows rather than the behaviour of individual vessels. Koldborg Jensen et al. [23] used a mathematical model to calculate the efficiency of a waterway, while Tassedra and Shoji [24] developed a framework to unravel the vessel traffic streams in Tokyo Bay. Queuing theory is another type of macroscopic model [25,26].

Macroscopic models, while good at scale, lack resolution to resolve the detailed causes of waiting times. Typically they also do not include realistic hydrodynamics, detailed accessibility policies, and berth availability information.

Mesoscopic models aim for a compromise where the behaviour of large numbers of individual agents can be simulated but their behaviour is aggregated to the level of objectively distinguishable events (e.g., mooring, (un)loading, unmooring, anchoring). This allows for a realistic representation of important port processes at scale while keeping computation times at acceptable levels. One of the first mesoscopic simulation models for port operations was developed by Hansen [27] and later expanded by Park and Noh [28]. These models focused mainly on land-based terminal operations, typically ignoring hydrodynamic aspects like currents and tides. Similar models were presented by Kondratowicz [29], Hassan [30], Demirci [31], Howard et al. [32], Arango et al. [33], Ugurlu and Yüksesky [34].

Mesoscopic simulation models with a more prominent focus on nautical traffic schematize the wet infrastructure as a network of nodes and edges, over which vessels sail and interact. An early model by Clark et al. [35] studied the Suez Canal, excluding port operations. Some later case-specific nautical traffic models that did include port operations did not include tidal restrictions, such as the work presented by Van de Ruit et al. [36] who studied the Maasvlakte of the Port of Rotterdam (PoR), and Yeo et al. [37] who studied the North Harbor of the Port of Busan. Furthermore, the models of Fransen et al. [38] and Nikghadam [39] focused on waiting times related to the availability of tugs and pilots in the PoR, but these approaches did not include downtime related to hydrodynamic restrictions.

More complete nautical traffic models with a clear focus on congestion and downtime were designed by Groenveld [40], whose HarbourSim model did consider the interactions between calling vessels and the port's infrastructure in detail, including terminals and (tidal) downtime. This model was applied to the Rio de la Plata in the work by Frima [41]. Moser et al. [42] created the similar HarborSym. Other comparable models were presented by Macquart [43], Rayo [44], Piccoli [45]. Tang et al. [46] developed a similar approach, albeit with a different process interaction-based approach. Furthermore, some case-specific nautical traffic models were constructed by Thiers and Janssens [47] for the Scheldt Estuary, by Almaz and Altioek [48] for the Delaware River, and by Scott et al. [49] for the Port of

Geraldton. Last, various in-house discrete-event models are known to exist in practice, such as DPCM<sup>®</sup> [50] and SiFlow21 [51], that claim to include detailed port congestion and tidal downtime, but no detailed information on these models is available in the open literature.

The use of Automatic Identification System (AIS) data to assess waiting times in port and waterway systems is a relatively new trend. Franzkeit et al. [52] and Ma et al. [53] focused on vessel waiting times in anchorage areas, Martinicic et al. [54] analysed arrival and turnaround times of vessels in the Port of Piraeus, Jafari Kang et al. [55] studied congestion in the Port of Houston, and Steenari et al. [56] investigated the performance of berths in the Port of Brest. A standalone AIS data analysis, however, is typically insufficient to unravel the detailed causes of vessel waiting times. This is due to the complex dependencies that exist between vessels and port infrastructure that cannot be deduced in full from AIS data alone without additional data and/or simulations [57].

Although most of the above-mentioned mesoscale nautical traffic models are, in principle, able to resolve the cascading effects due to congestion and (tidal) downtime, none of the openly available models simultaneously accounts for (1) realistic hydrodynamics, (2) detailed accessibility policies, (3) realistic vessel properties, (4) cascading effects of vessel-priority rules, (5) detailed waterway and berth layouts and (6) concrete berth-allocation policies. Also, none of the pre-mentioned studies provides a detailed decomposition of the causes for waiting times, let alone validates the predicted waiting times against actually observed vessel data. This paper addresses this gap by presenting a method that relies on a combination of data analysis and mesoscopic modelling.

We apply the method to a liquid bulk terminal in the 3rd Petroleumhaven (3rd PET) in the PoR. This terminal is expected to exhibit the above-mentioned cascading effects and involves vessels that govern the designed Maintained Bed Levels (MBLs) of the main access route. We analyse one year of AIS data, based on which we quantify vessel arrivals, laytimes in the anchorage and at the terminals, and vessel departures. Furthermore, we determine sailing speeds, turning times, and the effect of tidal restrictions. We subsequently adapt and use the open-source mesoscopic nautical traffic model OpenTNSim [58,59] to reproduce the observed vessels' behaviour through a hindcast study. The simulation allows us to analyse the effect of detailed hydrodynamics, Under Keel Clearance (UKC) regulations, reported vessel draughts, vessel-priority rules, waterway and berth layouts, and berth-allocation policies. We compare the predicted laytimes in the anchorage area with those observed in the AIS data, and unravel which causes contributed to these laytimes, accounting for tidal restrictions, congestion of port infrastructure, and priority in berth allocation. The approach improves our understanding of port performance, which in turn enhances our capability to suggest improvements to port operations and infrastructure (component) design.

Section 2 provides the details of the case study and the data sources. Section 3 describes the materials and methods used to set up and validate the nautical traffic model. Section 4 compares the model results to the AIS data and demonstrates the model's potential through a brief study of alternative MBL designs for the 3rd PET's entrance channel. Section 5 and Section 6 provide a discussion and our conclusions respectively.

## 2. Case Study

Before providing the details on the materials and methods in Section 3, we will introduce the case study in Section 2.1 and describe the data sources in Section 2.2.

### 2.1. Description of the 3rd Petroleum Harbour

The PoR is the largest seaport in Europe and serves as a transfer location of various types of cargo (mainly containers and liquid bulk) to other modalities bound for other destinations in Northern and Central Europe. An overview of the nautical infrastructure of the PoR is given in Figure 1. Sea-going vessels arrive at the port's Traffic Separation System (TSS) through which they sail to the port entrance, possibly visiting one of the anchorage areas. There are three routes to the port entrance. There is a west-east corridor (i), a north-south corridor (ii), and a north-west-north-east corridor (iii). The southern (northern) and

western (eastern) lanes are dedicated to inbound (outbound) traffic, while the deepest-draughted vessels make use of the central access channel, called the Euro-Maasgeul, and its dedicated anchorage areas. There are two deep-sea routes (A and B) that cross the TSS from north(-east) to south(-west).

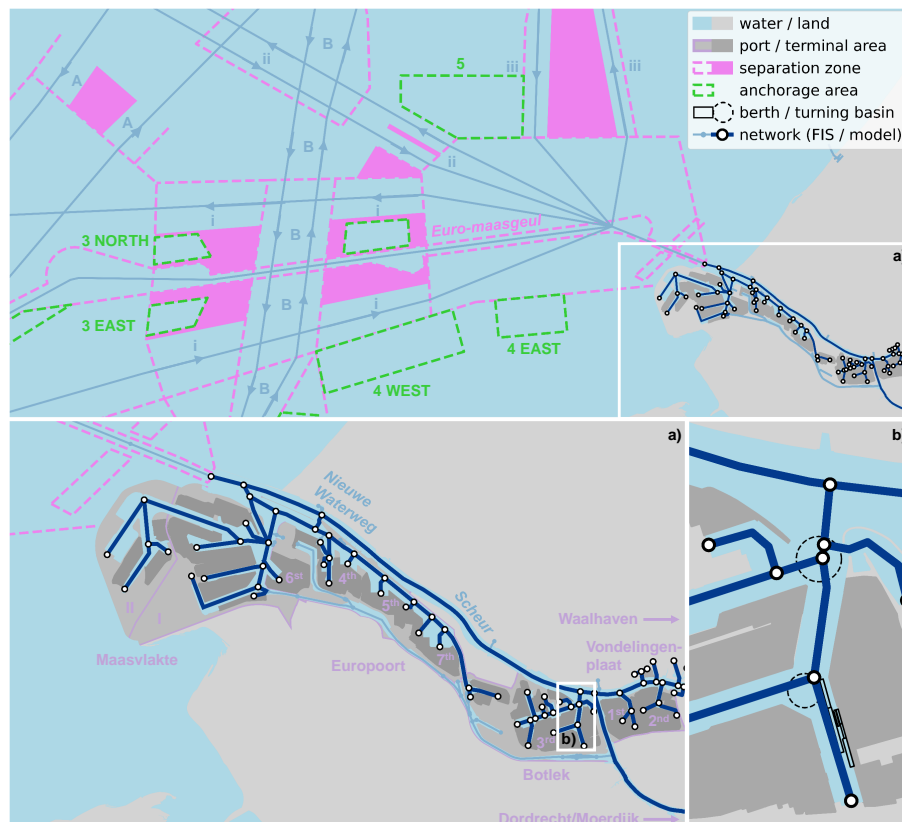


**Figure 1.** Nautical infrastructure of the PoR (a), including its TSS, and the 3rd Petroleumhaven (b). The TSS consists of three routes to the port (i, ii, and iii); two deep-sea routes are crossing the system (A and B).

The 3rd PET is an important transfer hub within the petrochemical cluster of the PoR. Constructed in the 1960s as part of the Botlek expansion, the basin is located along the main waterway, the Nieuwe Waterweg and Scheur (hereafter jointly called Nieuwe Waterweg), 21.5 km inland. Various terminals are located in the basin, facilitating both sea-going and inland vessels. The Botlek Harbour is an important hub as it defines the MBL of the NWW. In 2018, the NWW, and Botlek Harbour have been deepened from 14.5 m to 16.2 m to facilitate partially loaded New Panamax and Suezmax-type vessels up to a draught of 15.0 m. This research focuses on one of the liquid bulk terminals in the 3rd PET that operates these vessels. It has various dedicated jetties and quays for deep-sea vessels, coasters, and barges, with varying MBL and lengths.

To enter the 3rd PET, vessels are prone to a tidal restriction policy. The regulations regarding the vertical (water level) and horizontal (current) tidal policy are summarized in Table 1 and Table 2, respectively. During navigation over the NWW, a vessel is obliged to have an UKC of 10% of its draught, increased with a Fresh Water Allowance (FWA) of 1.0% of the draught up to halfway the waterway and 2.5% of the draught in the remaining part of the channel. The maintained bed level of the NWW is optimized for the deepest-draughted vessels [60], and varies from 16.2 m MBL in the first half to 16.4 m in the second half of the channel. Given this information, vessels with a draught of 13.0 m or more are prone to a vertical tidal window. Additionally, some vessels are prone to a horizontal tidal window when entering the 3rd PET. Vessels with a length equal to and greater than 180 m and a draught ranging from equal to and greater than 11.0 m (inbound) or 12.0 m (outbound)

up to 14.3 m are in principle only allowed to enter or leave when the tidal currents are less than or equal to 2.0 kn. Outbound vessels, however, are exempt from this condition during ebb tide, which is fully accessible. In contrast, vessels with a draught equal to and greater than 14.3 m are only allowed to enter or leave during flood tide when the currents are 0.5 kn and decreasing (ebb tide inaccessible).

**Table 1.** Restrictions for vertically tide-bound vessels to the 3rd Petroleumhaven based on entrance policy in the Port of Rotterdam.

	Nieuwe Waterweg		3rd PET
	KM 0–10	KM 10–21.5	KM 21.5
MBL	16.2 m	16.4 m	12.65–17.0 m
UKC	10.0% *	10.0% *	0.5 m
FWA	1.0% *	2.5% *	2.5% *

\* as percentage of the draught of the vessel in [m].

**Table 2.** Restrictions for horizontally tide-bound vessels to the 3rd Petroleumhaven based on entrance policy in the Port of Rotterdam.

Direction	Length	Draught	Tide	Condition
In	≥180 m	11.0 up to 14.3 m	Flood Ebb	2.0 kn 2.0 kn
Out	≥200 m	12.0 up to 14.3 m	Flood Ebb	2.0 kn accessible
In & Out	n/a	≥14.3 m	Flood Ebb	0.5 kn * inaccessible

\* only when currents are decreasing towards high water slack.

## 2.2. Data Sources

For this case study, we gathered the following data sources: geospatial, AIS, and hydrodynamic data. These sources are required for the underlying approach of this work (see Section 3).

### 2.2.1. Geospatial Data

Geospatial data is a collective term for all data with a specified geometry. For the approach discussed here, we are interested in a schematic representation of the port’s wet infrastructure.

On the one hand, this relates to the network of waterways that is schematized in the nautical traffic model as a graph, typically consisting of connected lines (edges) and points (nodes). Various geospatial processing tools, such as Shapely (<https://pypi.org/project/shapely/>, accessed on 13 May 2024), are available in Python to derive such networks from shapes that mark the fairways and water bodies. Moreover, spatial-temporal processing tools, such as the Python-based MovingPandas (<https://pypi.org/project/movingpandas/>, accessed on 13 May 2024), are able to derive networks by aggregating observed tracks in the AIS data (see Section 2.2.2). In many cases, more formal versions of such nautical traffic graphs exist. For the Netherlands, for instance, Rijkswaterstaat provides the latest information on the state of its waterways via the Fairway Information System (FIS) (<https://vaarweginformatie.nl/>, accessed on 13 May 2024). The network is also accessible in Bakker et al. [61]. This network follows the fairways with sufficient detail and is therefore used in the case study of the 3rd PET (see Figure 1).

On the other hand, this relates to information on important port infrastructure, such as anchorage areas, fairways, turning basins, and berths. Generally, it is sufficient to specify such infrastructure in the form of shapes that specify their position and outline. In some cases further metadata are needed, e.g., the capacity of an anchorage area or berth, the applicable UKC policy for a fairway section. Port authorities may also have accurate geospatial

datasets including metadata that can be used. In this research the geometric extents of the 3rd PET, the PoR and the areas of the TSS (see Figure 1) were obtained from OpenStreetMap (<https://www.openstreetmap.org/>, accessed on 13 May 2024) using the open data mining tool Overpass turbo (<https://overpass-turbo.eu/>, accessed on 13 May 2024). A polygon containing a specific area between the breakwaters, used in the AIS analysis in Section 3.1.1, was created using GoogleEarth. Specific geospatial data with metadata on MBL and FWA was obtained via PoR, through its Port Map application (<https://experience.arcgis.com/experience/0127b94d675f48dd80702b5b81be6020/?draft=true&org=portofrotterdam>, accessed on 13 May 2024). The geospatial data of the PoR are reliable, as they are used in daily operations. The data of OpenStreetMap were carefully validated using satellite imagery. While the geospatial data of the PoR are confidential, the open-source data are shared in Bakker et al. [61].

### 2.2.2. AIS Data

The AIS is an automatic vessel tracking system that is primarily used to guarantee safety in waters with heavy traffic. It consists of time series of various types of messages that contain either static vessel properties (e.g. the vessel's unique Maritime Mobile Service Identity (MMSI) number, the vessel type, the vessel's dimensions) or dynamic vessel properties (e.g. location, Speed Over Ground (SOG), Course Over Ground (COG)). The dynamic data are transmitted with a higher frequency than the static data; every 2–10 s a message is transmitted for a sailing vessel, increasing to 180 s for an idle vessel. By combining the static and dynamic components, the transit information of each individual vessel can be gathered, stored, and researched. Raw AIS data are available in National Marine Electronics Association (NMEA) encoding. The open-source Python package PyAIS (<https://pypi.org/project/pyais/>, accessed on 13 May 2024) can be used to decode these raw data and convert them into readily usable dataframes (i.e., Pandas <https://pypi.org/project/pandas/>, accessed on 13 May 2024). Ready-to-use, pre-decoded, and cleaned AIS data products may in some cases be available from organisations like the Coast Guard, the local water authority, and port authorities. For this study, AIS data for the whole area of the PoR (including the TSS) for the entire year of 2019 were provided by Rijkswaterstaat. They decoded and anonymized the data, and guaranteed its quality by extensive error removal. The anonymization algorithm ensured that the vessels maintained a unique vessel ID. The data processing that was applied to these AIS data is discussed in Section 3.1. Although the data are confidential, the derived input data for the model can be accessed through Bakker et al. [61].

### 2.2.3. Hydrodynamic Data

Hydrodynamic data are required for the calculation of the vertical (water levels) and horizontal tidal windows (current velocities), where and if applicable. The data can furthermore be used to determine the vessels' sailing speed over water. A useful data source should specify this hydrodynamic data as a function of time in at least two strategic locations. Data from measurement stations could be interpolated to relevant locations, e.g., to key nodes of the nautical traffic network. More measurement stations increase the accuracy. Another option, that is applied in this research, is the use of a well-calibrated and validated hydrodynamic model. The PoR makes current hydro-meteo data available via its Weather, Tides and Water Depths platform (<https://www.portofrotterdam.com/en/up-to-date-information/weather-tides-and-water-depth>, accessed on 13 May 2024). An important tool in this platform is the Operationeel Stromingsmodel Rotterdam (OSR) that calculates water levels and currents, while constantly being re-calibrated with the most recent measurement data. This numerical model calculates the present hydrodynamic situation and makes a 24-h prediction on a daily basis. Furthermore, hindcast simulations can be made with the model, which was done for this study. Hydrodynamic data on relevant locations was acquired by adding monitoring points to the model's computational grid. The confidential model output was made available in NetCDF-files for further processing. The quality of

the water level and current velocity data of the OSR can be guaranteed as the model is calibrated extensively up to a level that it can be used confidentially in daily operations.

### 3. Materials and Methods

To decompose the waiting times for the liquid bulk terminal in the 3rd PET harbour in the PoR we apply a mesoscale simulation model to hindcast a period for which observed AIS data are available. The following information is required for the model set up:

- a geospatial graph of the port network, including:
  - schematizations of relevant port infrastructure,
  - governing UKC policies,
  - priority rules and berth-allocation policies; and
- the calling vessels in the form of agents, including:
  - dimensions (i.e., length, beam, and draught), and
  - followed trajectories to derive:
    - \* origin-destination information,
    - \* speeds, and
    - \* laytimes in various port areas; and
- realistic hydrodynamics over the port network, including:
  - tidal elevations as a function of time and space, and
  - current velocities at critical locations.

The required information can be derived from available geospatial data, AIS data, and hydrodynamic data (see Figure 2).

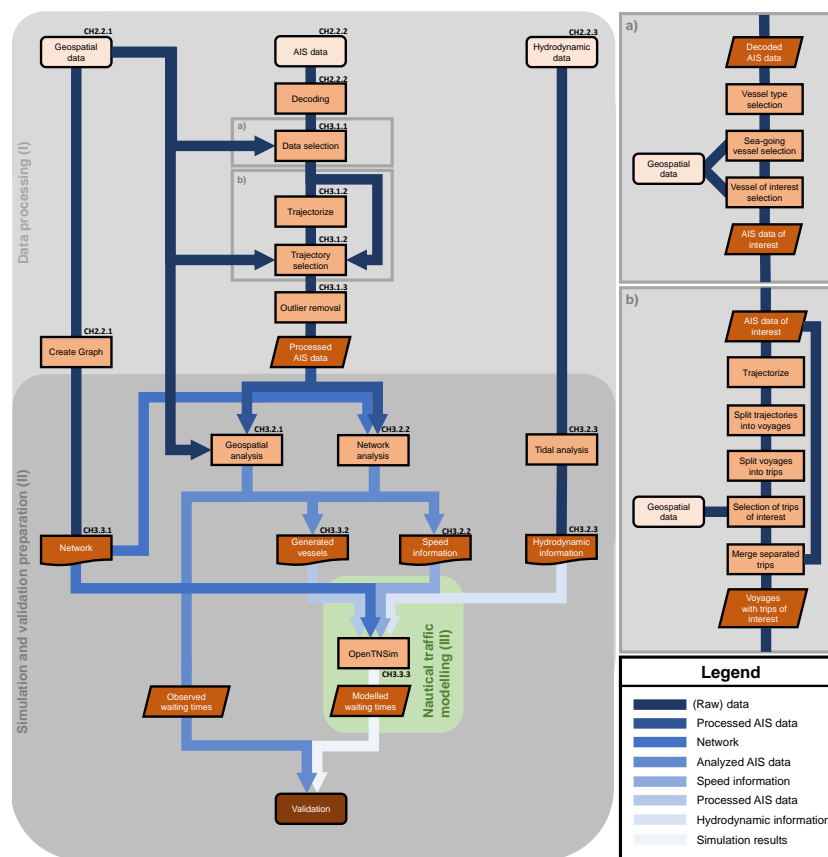


**Figure 2.** Information flows for the set up and validation of the nautical traffic model, consisting of data processing (I), simulation and validation preparation (II), and nautical traffic modelling (III). Close-ups (a,b) respectively schematize the processing steps in the the selection and trajectorisation of the data. The symbols are according to the ISO standards.



Section 3.1 describes processing steps applied to the AIS data (Figure 2I). Section 3.2 describes the additional steps that are needed for simulation and validation (Figure 2II). Section 3.3 describes the nautical traffic model that was applied (Figure 2III).

### 3.1. Data Processing (I)

The decoded AIS data contain information on all types of vessels, including barges, and tugs and pilot boats which constitute the majority of the data received. For our study, we are primarily interested in the behaviour of sea-going cargo vessels. To arrive at the desired level of detail the AIS data had to be filtered and trajectoryised, and outliers had to be removed. For this sequence of algorithms, we followed the basic principle of performing the most computationally demanding algorithms on as little data as possible. The processing was performed using the multi-core Planetary Computer of Microsoft (<https://planetarycomputer.microsoft.com/>, accessed on 13 May 2024). The data-processing steps are described in the subsequent subsections and are published in Bakker et al. [61].

#### 3.1.1. Filtering of the AIS Data

Figure 2a shows some first filtering steps that were applied to arrive at the AIS data of interest. By filtering on vessel type, we reduced the overall dataset to cargo vessels and tankers. Next, we used a polygon encompassing the access channel between the breakwaters through which inland barges will not sail. This allowed us to further trim down the dataset to only the sea-going cargo vessels that call at the port. A combined polygon encompassing the berths of the specific liquid bulk terminal in the 3rd PET was used to select only those sea-going vessels that called at the liquid bulk terminal at least once during the entire year of 2019.

#### 3.1.2. Trajectoryisation into Trips and Voyages

Next, Figure 2b shows the subsequent steps that were taken to process the AIS data. First we ‘trajectoryised’ the now filtered AIS data based on a unique static vessel property (i.e., vessel name). For each vessel, this resulted in a tabulated chronological overview of all time-position combinations in the 2019 AIS data. For each time-position combination, instantaneous vessel properties like speed, heading, and acceleration were added to the table for later use.

Since the total trajectory of one vessel for a given year generally consists of several voyages (or port calls) that in turn can consist of multiple trips (origin-destination combinations), the next processing step is to split the vessel trajectories into ‘voyages’ and ‘trips’.

A ‘voyage’ (or port call) is defined as a vessel’s in- and outbound time-of-stay within the port infrastructure, including the TSS. To distinguish between voyages we made use of a time gap without any messages in a vessel’s trajectory data. The open-source Python package MovingPandas (<https://pypi.org/project/movingpandas/>, accessed on 13 May 2024) provides the so-called ObservationalGapSplitter method for this purpose. We used a gap of 6 h to distinguish between voyages in a vessel’s trajectory data. Each individual voyage was assigned a unique ID for purposes of later analysis.

A ‘trip’ is defined as a subset of a vessel’s trajectory (or voyage) data that can be demarcated by a clear origin and destination. The start and stop of each voyage are taken as origin and destination, respectively. To distinguish between trips within each voyage we made use of the time that a vessel stays at a fixed location. The StopSplitter method of MovingPandas (<https://pypi.org/project/movingpandas/>, accessed on 13 May 2024) can be used for this purpose. It creates splits based on the condition that a vessel stays within a certain radius for a minimum duration. Based on trial-and-error we used a diameter of 25 m and a minimum duration of 30 min to identify intermediate stops in each voyage. Each individual trip was assigned a unique ID for purposes of later analysis.

As the StopSplitter operation proved to be time-consuming, we separated the trajectory data of each vessel into sub-sets of roughly equal size. This allowed for parallel processing, which greatly reduced the processing time. One artifact of this approach, however, was

that artificial splits were created at the boundaries between the sub-sets. To resolve this, a merge step was required to rejoin sub-trips that belonged together. Another artifact was that the StopSplitter method deletes the trajectory data that fall within its search radius. As a consequence, the start and end points of subsequent trips would no longer match. In some cases, this caused significant shifts in a vessel's position from the end of one trip to the start of the next, which in turn caused problems in the subsequent analysis. To resolve this issue, the deleted data were retrieved and restored.

To focus on the in- and outbound traffic of the 3rd PET, we used the combined polygon of the 3rd PET berths to reject all trips that did not stop or start in this area. The remaining trips were sorted based on their start time, classified as in- or outbound depending on their start- and endpoint, and combined into round trips. If the inbound trip had one of the anchorage areas as its origin, the preceding trip that had this anchorage as its destination was added to the round trip. This resulted in 255 individual ships that undertook a total of 481 unique voyages, consisting of one or two inbound trips to the 3rd PET (depending on whether the vessel laid in one of the anchorage areas) and a single outbound trip from this terminal. Vessel properties such as length, beam, and draught, as derived from the AIS data, were added to each trip dataset. The difference in draught between the in- and outbound trips was added as the (un)loading quantity to each voyage.

### 3.1.3. AIS Data Outlier Removal

Unfortunately, AIS data are known to contain errors. Some of the AIS fields rely on manual input, so human error is to be expected here. But other fields rely on sensors, such as the vessel's location as a function of time, as well as its SOG, COG, and derived speeds and accelerations. The last data-processing step is to remove errors in this latter kind. Since this is a very time-consuming row-by-row operation this step was performed at the very end on the minimum subset of relevant voyages and trips. The following four conditions for sailing vessels, proposed by Abreu et al. [62], were used to classify whether a data point was considered anomalous: stop, drift, acceleration, and turning. Based on trial and error the condition for sailing vessels was set to a speed of 2 kn minimum. Suspected outliers were removed accordingly.

## 3.2. Simulation and Validation Preparation (II)

The processed data from the previous subsection (I) can now be used to generate inputs for the nautical traffic simulation and validation. The details of the data-analysis steps are provided in Bakker et al. [61].

### 3.2.1. Origins, Destinations and Other Trip Data

The 'real world' coordinates of origins and destinations can be extracted straightforwardly from the voyage and trip datasets. Next to origins and destinations, each simulation needs at least the following information for each calling vessel: arrival time, sailing speeds along the route, projected turning time in the turning basins, designated berth(s), and the (un)loading time at the berth(s). Also, the vessel's actual laytime at the anchorage area must be recorded to validate the simulation results.

The designated berths of call are determined using the stoppage data between the in- and outbound 'trips'. An algorithm counts the number of AIS points that fall inside the different berths and selects the berth with the most hits as the vessel's most likely berth of call. The unloading times at these berths are estimated from the stoppage intervals between the in- and outbound trips. The time for (de)berthing is assumed to be included in these intervals.

Turning times are estimated with an algorithm that determines the time of stay in the turning basins that the sailing vessel passes during its voyage. The algorithm selects the turning time with the maximum time of stay, as the vessel only needs to turn once during its voyage. This may be during its inbound or outbound trip.

The laytimes in the anchorage areas are determined similarly to the unloading times at the berth, though with the start time of the second part of an inbound trip and the end time of the first inbound trip, starting and ending in the anchorage area respectively. If the vessel did not visit an anchorage area, the laytime is set to zero.

### 3.2.2. Mapping Locations to the Graph

The nautical traffic model requires the origin and destination nodes for each trip, rather than the 'real world' coordinates, to enable routing on the network graph.

To map the trajectories of the AIS trips onto the routing graph we used an algorithm that finds the nearest directional edge in the graph for each coordinate of the trajectory. Since this is a time-consuming operation for large amounts of data and complex, extensive networks, the algorithm was initially only applied to special way-points. These way points were derived based on a running criterion on cumulative distance (1000 m) and cumulative course difference (30 degrees). Based on the identified nearest directional edges of two consecutive way-points, a significantly smaller sub-graph could be defined, which was used for the search of the nearest directional edge for the coordinates between those way-points.

The origin and destination nodes of the trips were determined through a similar nearest-node algorithm. Accordingly, the timestamp of the AIS message closest to the origin node of the first trip was set as the arrival time at the port of the vessel. As vessels may originate from, or are bound for, another location within the port, the origin and destination of a voyage are not necessarily at the TSS. Since we decided to omit the modelling of traffic in the TSS (see Section 3.3.1), for those vessels that did arrive from, or depart to, this area we decided to set the origin (including the arrival time) or destination to the node at the port entrance between the breakwaters. The observed arrival times of the vessels at this newly defined port entrance are of vessels that were cleared by the vessel traffic service to enter the port, as vessels originating from the TSS will wait in an offshore anchorage area for a tidal window and berth availability. Hence, to be able to quantify and resolve the waiting times in the anchorage areas, the arrival times had to be corrected (brought forward) for the time that the vessel waited in the anchorage area. Thus, if a waiting time is required for a vessel it will be ordered to wait at the port entrance in the nautical traffic model.

Now that the actual routes of the vessels are mapped onto the graph, we can identify speed distributions for each individual directional edge that was covered by the vessels of call. For the simulations in this study, we assumed, that vessels maintain their average speed over the edges. However, since the routes on the graph and AIS trips do not map exactly in space, the actual average speed of the vessel differs from the average vessel speed over the edge. For this study we concluded that the vessel's average speed over the edge would be the most accurate, meaning that the edge length and arrival time at and departure time from the edge are used to determine the average network speeds. This information was added to the graph so that it would be available for the vessels during the simulation. The vessel speed over the network is important in the calculation of the tidal windows. The slower the vessel sails, the smaller these windows will be.

### 3.2.3. Adding Tidal Information to the Graph

Next to speeds, the simulations also require hydrodynamic data to be available on the network's nodes to enable the determination of tidal windows. Table 1 shows that different tidal restrictions apply for flood and ebb tidal periods. Determining the start and end times of these flood and ebb periods in astronomic tidal hydrodynamic data requires a tidal analysis. We performed a Fourier analysis on the water levels and current velocities, and a (preceding) Principal Component Analysis (PCA) on the current velocity magnitudes and directions. The tidal component analysis is performed using the Hatyan package (<https://pypi.org/project/hatyan/>, accessed on 13 May 2024). The tidal periods were derived based on the intersection points of the abscissa (current velocity magnitude = 0 kn), i.e., the slack tides.

### 3.3. Nautical Traffic Model (III)

For our nautical traffic simulations we used the open source Python package OpenTNSim (<https://pypi.org/project/opentnsim/>, accessed on 13 May 2024), which is an agent-based discrete-event simulation package that is based on SimPy (<https://pypi.org/project/simpy/>, accessed on 13 May 2024). OpenTNSim provides a library of standardised ‘mixin’ classes that can be combined to create agents or infrastructure components with user-specified properties and behaviour.

Adding the ‘Identifiable’ mixin to an agent, for example, allows the user to give that agent a name and/or a Universal Unique Identifier (UUID). Adding the ‘Movable’ mixin gives that agent the ability to move at a predefined speed. The ‘Routeable’ mixin, which implies ‘Movable’, allows an agent to move over a graph following a specified route with an origin, intermediate waypoints, and a destination. The ‘VesselProperties’ mixin allows the user to specify agent properties, such as length (L), beam (B), draught (T), payload, etc. The ‘Log’ mixin ensures that key information is logged for later inspection.

The same mixins can be used to define infrastructure components in the transport network. Components like anchorage areas, turning circles, berths, jetties, quays, etc. can be named by adding the ‘Identifiable’ mixin. The user can furthermore specify how many vessels can make use of that object at the same time by adding the ‘HasResource’ mixin. If the maximum number has been achieved, i.e., a jetty can handle one vessel at a time and is already occupied, then the next vessel that wants to call on that jetty has to wait until it is available. Waiting is typically done in one of the ports anchorage areas.

Specifically for this study, we developed various new mixins. Most noteworthy are the VesselTrafficService-mixin and a PortInfrastructure-mixin. When these mixins are added to an object, it allows to request information from a port authority, i.e., regarding the availability of a berth, and the availability of a tidal window. The mixins communicate berth availability in advance, meaning that a vessel can already enter the port to sail to their berth of call when a vessel that is occupying this berth is scheduled to leave before the arrival of the next vessel.

The minimum required input for a simulation consists of the port infrastructure network and the generated vessels with their routing information and realistic properties. To achieve this paper’s aim we added the following specifics to the network: the detailed accessibility policies that apply at the different edges (i.e., tidal restrictions, vessel-priority rules), the average vessel speeds per edge, and the hydrodynamic data at key nodes to determine when vertical and horizontal tidal windows are available. The details of the nautical traffic simulation are discussed according to Figure 3. The derived input data (apart from the hydrodynamic data), set up and implementation of the model can be consulted in Bakker et al. [61].

#### 3.3.1. Port Infrastructure Network

The waterway network in Figure 3 was extracted from Rijkswaterstaat’s FIS that includes the PoR area (see also Figure 1). For simplicity, the TSS was not included. The complex vessel behaviour in the TSS is challenging to mimic and does not affect the waiting times of the vessels that sail to the 3rd PET. Since the TSS contains (the routes to) the anchorage areas, we placed a virtual anchorage at the port entrance to serve as the vessel waiting area. Vessels originating or departing to the TSS were modelled to be bound from/to the port entrance between the breakwaters. The arrival times of the vessels were corrected accordingly (see Section 3.2.2).

The port infrastructure that was added to this network consists of the port entrance on the most seaward node with the virtual anchorage area, the waterways towards the Botlek area schematised as nodes and edges, the dedicated turning basin for the 3rd PET (for vessels up to a length of 290 m) on the penultimate node, and the liquid bulk terminal in the 3rd PET on the last edge with its various berths for sea-going vessels. The turning time does not contribute significantly to the total turnaround time, however, vessels waiting for

other vessels to turn or to pass the turning basin before they can turn can slightly contribute to the waiting times of the vessels.

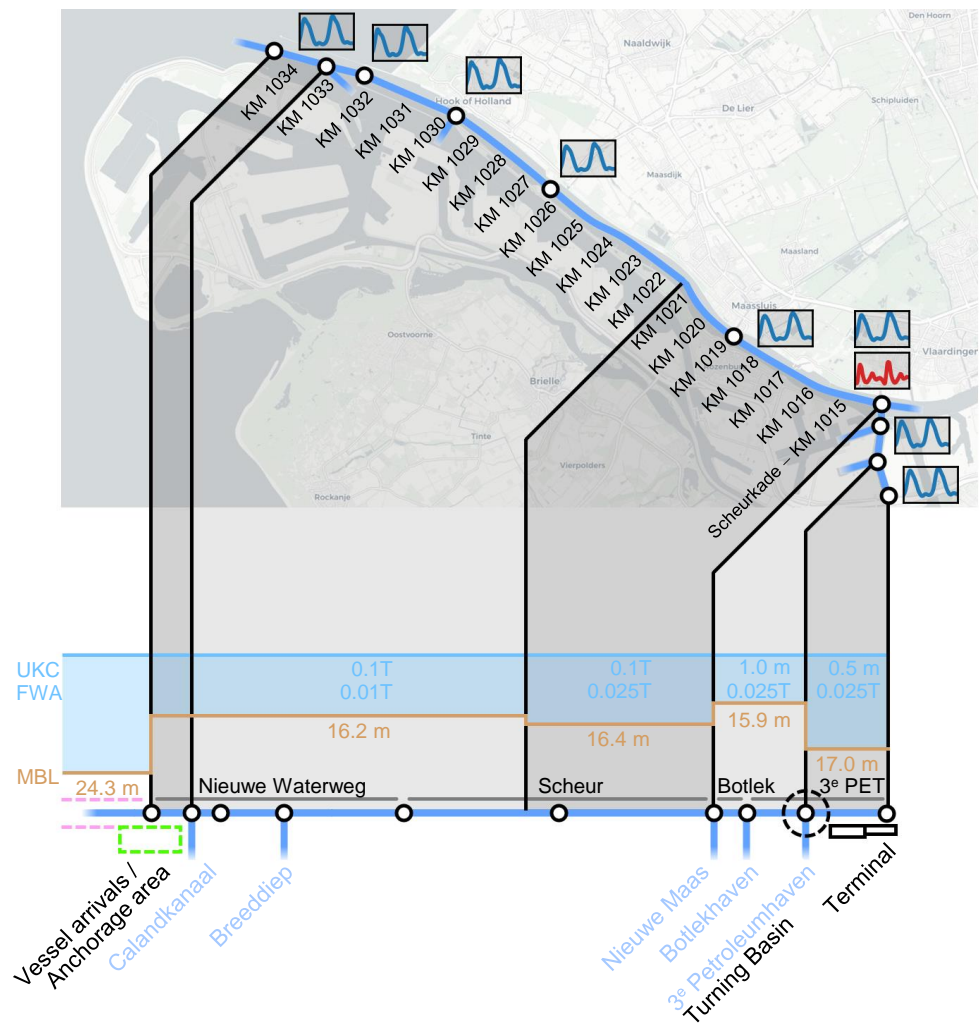


**Figure 3.** Overview of the nautical traffic model based on an extraction of the graph following the route to the 3rd PET. The MBL, UKC, and FWA policies are added, which may be constant or dependent on the draught (T) of the vessel. The water levels (blue time series) and current velocities (red time series) are added to the nodes of the network.

Key properties of these objects were specified using the OpenTNSim mixin classes. Anchorages, waterways and turning basins were modelled using the ‘HasResource’ mixin. The virtual anchorage area is assumed to have an infinite capacity to prevent vessels from entering the anchorage area and leaving the port without being processed. The waterway edges were also assumed to have an infinite capacity, and they were modelled as bi-directional edges to account for two-way traffic. It was assumed that a safe distance is maintained by the vessels so that encountering does not lead to a reduction in speed. Overtaking by the sea-going vessels is assumed not to occur, as these vessels are sailing over the network with similar speeds. The turning basin can handle one vessel at a time, and the manoeuvre of the vessels is modelled to occur during the inbound trip. Outbound vessels can still occupy the turning basin, as they have to pass through it when leaving the port. The berths of the liquid bulk terminal are modelled using the FilterStore class from SimPy (<https://pypi.org/project/simpy/>, accessed on 13 May 2024) [3]. This concept works as a store of products (berths) with each their own properties, such as a name, a MBL, and a maximum ship length that they can operate. The liquid bulk terminal has a few quays that do not have a unit capacity, like jetties, but that have a finite length. These quays,

however, contain a limited number of fixed pumping facilities and are therefore modelled similarly to jetties. For simplicity, we assume empty berths at the start of the simulation.

Water level data were added to relevant nodes, and the governing MBL and the UKC policies were added to the edges (see Figure 3). Current velocity data were included at the critical point along the route where the vessels turn (KM 1015 at the Scheurkade). The water level and current information are used to calculate the tidal windows according to the governing rules that are summarized in Table 1.

### 3.3.2. Generated Vessels

For our model implementation, vessels have to be generated with the following required information:

- length and draught per trip in the voyage,
- origin, intermediate waypoints and destination nodes that constitute the route of the voyage and trips over the network,
- arrival time at the vessel's origin node,
- designated berth(s) of call,
- turning time in the turning basin,
- the (un)loading time(s) at the designated berth(s), and
- the change in draught at the berths.

Since we perform a hindcast study, we replicate the observed traffic using the processed AIS data (see in Section 3.2). Each vessel travels past the nodes that are specified in its route. Between these specified nodes the route is determined with Dijkstra's shortest path algorithm if needed. The route leads to the designated berth. In reality, berths can be assigned freely based on their properties and restrictions that prevent small vessels from berthing at the deep-sea berths (e.g., a minimum vessel length or draught requirement), which also could have been included in the model.

### 3.3.3. Modelling Strategy

After the port infrastructure network and the generated vessels have been specified, SimPy (<https://pypi.org/project/simpy/>, accessed on 13 May 2024) works out how these vessels, together, move through the network. The simulation resolves where and when which vessel needs to wait and for how long. Waiting times in the anchorage area will occur if a vessel has to wait on either a tidal window or unavailable (congested) port infrastructure, either directly or indirectly through cascading effects. Priority rules to be included in the berth planning strategy to minimize the demurrage costs of vessels were omitted in this research but can be included in the model. Instead, the sporadically observed behaviour of newly calling vessels jumping ahead in the queue, over already waiting vessels, was mimicked by giving additional waiting times to these latter vessels. This waiting time equalled the difference between the arrival time between the two vessels and was presumed to be due to the priority rules. To quantify the individual contributions of the tidal restriction, berth unavailability and priority rules to the waiting times of vessels, as well as the cascading effects of these causes, the simulation was also run without tidal windows and prioritization. Besides the reference situation, the model is applied to test alternative MBL designs for the NWW.

## 4. Results

We first describe behaviour that can be observed in the AIS data. Next, we describe the results from the hindcast made with the nautical traffic model.

### 4.1. AIS Data

The processed AIS data are visualized in Figure 4. A total of 481 voyages were identified, made by 255 different vessels. 52.8% of these voyages were operated by vessels that can be classified as coasters, while 23.1% were of the Handysize class, 9.1% of the Handymax class, and 12.5% were vessels of the Panamax class. Only 2.3% of the voyages

were made with New Panamax-class vessels and a single Suezmax-class vessel called at the terminal. From this dataset, we could also derive origin-destination patterns and length-draught distributions. For example, 80.7% of the inbound trips used the NWW, of which 5.2% is tide-bound (83.3% of the total tide-bound vessels). Figure 5 shows histograms and distributions for a number of key aspects of the observed traffic: laytime at the offshore anchorage areas, sailing times for inbound and outbound vessels over the NWW, turning times for inbound and outbound vessels, and laytime at the terminal. Figure 6 shows the distribution of speed over the network for vessel voyages that called at the liquid bulk terminal.

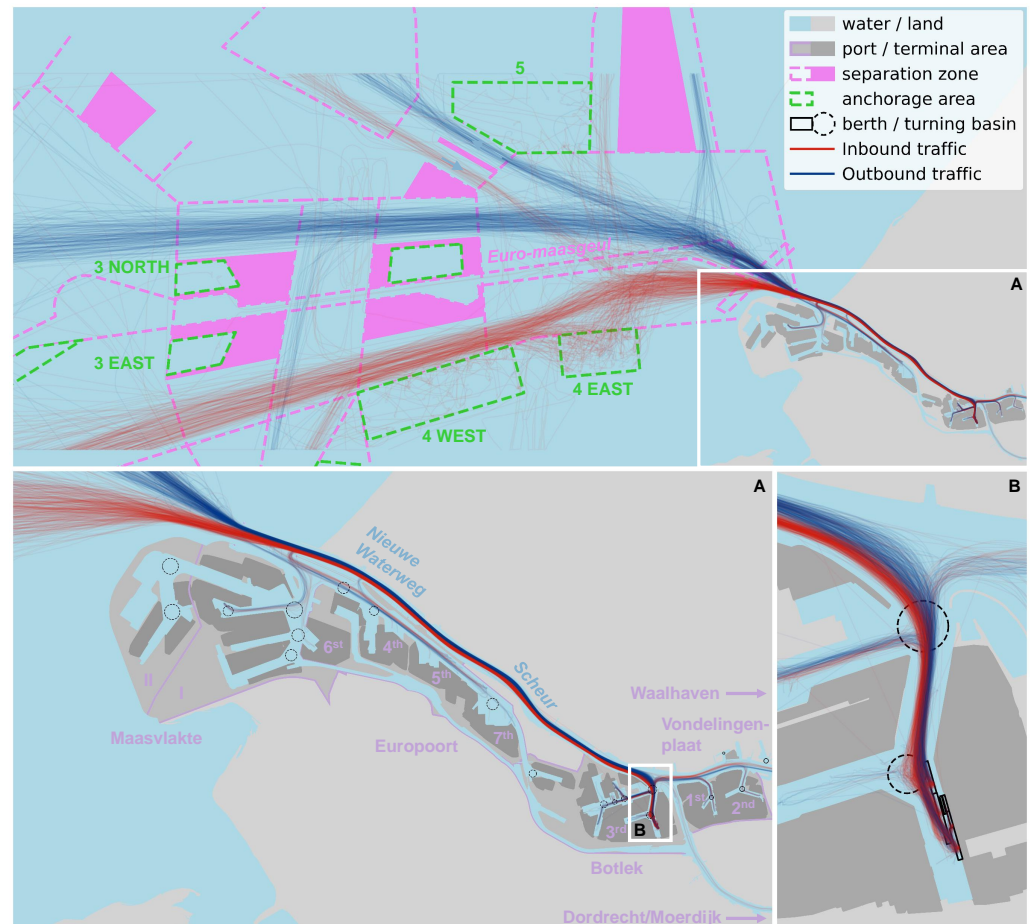


**Figure 4.** Overview of the processed AIS data: inbound and outbound vessels are shown that are navigating the TSS. Two close-ups are added of the trips’ track through the NWW (A) and the 3rd PET (B).

#### 4.1.1. Laytime at the Anchorage

The laytime of vessels at the anchorage area will be used to validate the model. 39.7% of the voyages included laytime in the anchorage area. 89.5% of these voyages originated from offshore. Based on expert judgment, it is expected that voyages originating from other areas in the Port of Rotterdam claim internal anchorage areas or, less likely, wait at their terminal, and only visit an offshore anchorage area if the internal anchorage areas or terminal are not available or waiting in internal anchorage areas is impossible. Furthermore, 59.7% of the voyages with laytime in an anchorage used the closest anchorage to the port along their route, 4 EAST. 88.4% of these voyages arrived from the southwest. 13.1% of the voyages with waiting time used anchorage 5, of which all vessels from offshore arrived from the northwest. Out of the deepest-draughted vessels ( $14.8 \text{ m} \leq \text{draught} \leq 15.0 \text{ m}$ ) the four New Panamax-class vessels were obliged to navigate the Euro-Maasgeul. Two of these vessels had a laytime in the dedicated anchorage areas of 3 North and 3 South.

From the probability density function (pdf) in Figure 5a, we observe that 56.5% of the voyage that had laytime in the anchorage area did not wait for more than a day. Voyages with larger vessels tend to wait shorter, as only 29.2% exceed a laytime of a day. The longest observed laytime was found for a New Panamax class vessel that waited over 13 days. The second longest was found for a Coaster that waited almost 5 days. Such long laytimes of over 2 days occurred frequently for voyages with smaller vessels (16.2%).

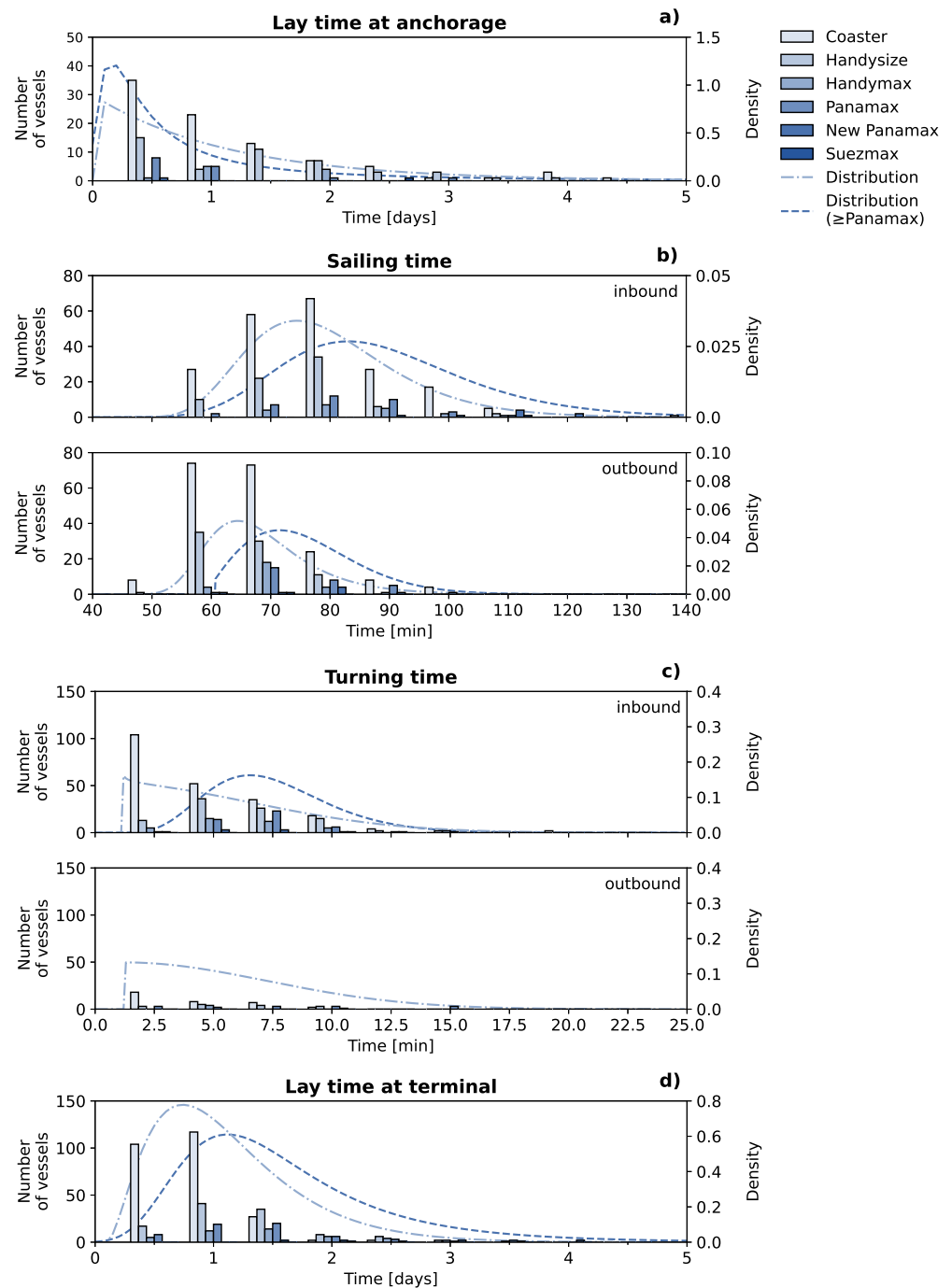


**Figure 5.** Histograms and distributions of the calibration data derived from the processed AIS data: laytime at the offshore anchorage areas (a), sailing time for inbound and outbound vessels over the NWW and Scheur (b), turning time for inbound and outbound vessels (c), and the laytime at the terminal (d).



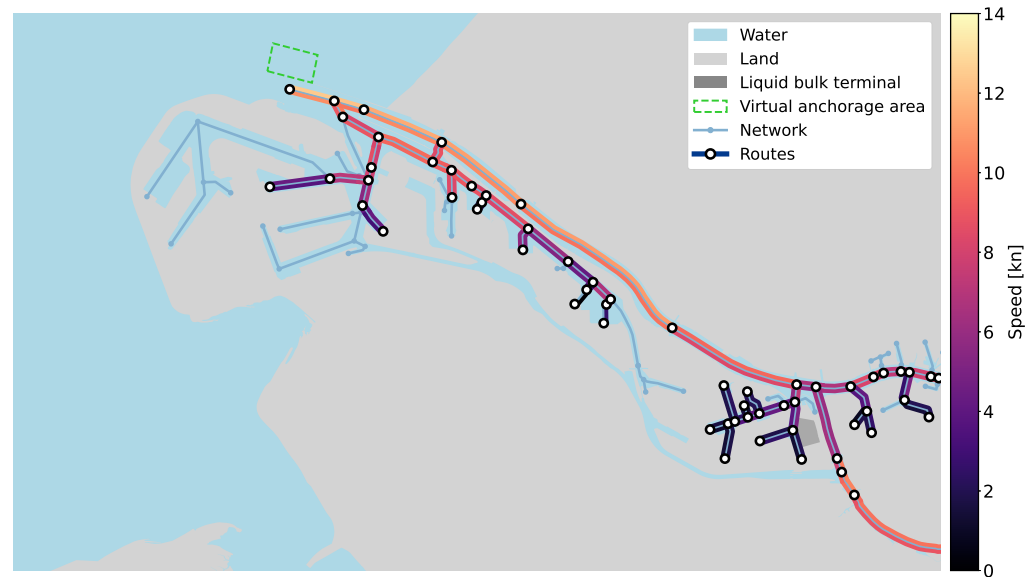


**Figure 6.** Speed distributions over network derived from mapped AIS data of the vessel voyages that called at the liquid bulk terminal. The coverage of the network corresponds with the tracks found in Figure 4.

#### 4.1.2. Sailing Time

The sailing time over the NWW, presented in Figure 5b, is important to estimate the delay in arrival time at the terminal and to determine the tidal windows in the model. We observe that the speeds contain significant spreading with transit times ranging from 50 to 120 min. We observe that inbound vessels, on average, sail with lower speeds than outbound vessels; the modal traveling times are in the order of 75 and 65 min, respectively. This bias may be because most trips occurred during ebb tide, as well as that outbound vessels on average had less draught; larger vessels were observed to sail with lower speeds than smaller vessels with modal differences of around 10 min. However, a clear correlation between the tide and the sailing speed was not found. Observed variation is expected to be due to captain behaviour, ambient traffic, the strength of (tidal) currents and winds, etc.

The above-mentioned behaviour can also be observed in the average in- and outbound speeds over the network as visualised in Figure 6. Over the NWW and the Scheur the average vessel speed is nearly constant: 9.9 knots for inbound vessels and 11.1 knots for outbound vessels. Towards the Botlek and the New Meuse, the average speeds drop due to decelerating (from 8.3 to 5.9 kn, on average) and accelerating vessels (from 7.4 to 9.5 kn, on average) that are sailing in and out of the Botlekhaven, respectively. The contrary holds for the entrance of the Port of Rotterdam, in which outbound vessels seem to accelerate further to 12.5 kn. Inside the harbour basins the average speeds are low, below 5.0 kn (in the 3rd PET), as expected, and decreasing further towards the ends of the harbour basins as a consequence of the vessel manoeuvres.

#### 4.1.3. Turning Time

Figure 5c shows the turning times of the vessels of call, i.e., when a vessel is occupying the entrance to the terminal and inhibits other traffic from entering/leaving the 3rd PET. They range from a minute up to tens of minutes with a maximum of 43 min (not shown in the figure). However, from the pdf, we can observe that 91.1% of the voyages have a turning time of less than 10 min. The turning times of vessels larger than coasters follow a positively skewed distribution with a modal duration of around 6 min. Most vessels (84.2% of the total) turn during their inbound trip, which is according to common practice, as this was previously mandatory based on safety regulations. There is no significant increase in the modal turning time with vessel size, although the longest turning times are observed for larger vessels. Most probably, the outliers are caused by severe winds. Since coasters

are more manoeuvrable, most of these vessels are believed not to turn at the turning basin, but rather manoeuvre at the berth, thereby passing the turning basin without actually turning. They affect the overall distribution severely.

#### 4.1.4. Laytime at the Terminal

The observed time at the berth of the vessels is presented in Figure 5d. Note that during this time, the vessel occupies the berth during which other vessels cannot make use of this berth. The pdf follows a positively skewed distribution with a lot of spreading ranging from a few hours to several days. The modal laytime of all vessels of call is slightly longer than a full day. For smaller vessels, especially coasters, the distribution shifts more to shorter laytimes of around half a day, while for the largest vessels (Panamax class and larger) the distribution shifts to longer times with a mode of around one-and-a-half day. Understandably, these differences are caused by varying transshipment volumes of liquid bulk between the vessel and the terminal that increase with vessel size. The standard deviation, however, is large compared to the average laytime for all types of vessels. Based on expert judgment, this is presumably caused by varying onboard pumping capacities and the number of storage compartments that need to be (un)loaded.

#### 4.1.5. Tidal Restrictions

Figure 7 shows the draught and length combinations of the incoming and outgoing vessels of call at the liquid bulk terminal. Only 4.9% of the inbound trips were prone to tidal windows during the voyage, while none of the outbound voyages were affected by a tidal window. During 83.3% of these trips, vessels had long-lasting horizontal tidal windows, based on a critical velocity. Only for 10.0% of these vessels (with a draught greater than and equal to 13.0 m), the tidal windows started to be shortened further by the vertical tidal constraint. For these vessels, the accessibility was, however, fully determined by the criterion of the critical tidal velocity. The resulting tidal windows, combining the vertical and horizontal tidal windows, are visualized in Figure 8a for a vessel with 14.2 m of draught. For vessels with such (deeper) draughts, the horizontal tidal windows are severely (more) shortened by the vertical tidal constraint. This combination still resulted in adequately long tidal windows. 16.7% of the inbound trips that are restricted by the tide were prone to a narrow tidal window, consisting of a strict, governing point-based horizontal tidal window within a tight vertical tidal window (see Figure 8b). Only during 0.6% of the inbound trips, vessels were observed to have the maximum design draught of 15.0 m, which had to fully exploit the MBL design of the NWW, Scheur, and the Botlek, including the 3rd PET. Based on the observation that the most deep-draughted vessels left the terminal with less draught, we can consider the terminal to be an import terminal. This claim is, moreover, further signified by the fact that most incoming coasters (up to a draught of 8.6 m and a length of 120 m) arrive with less draught compared to their departure.

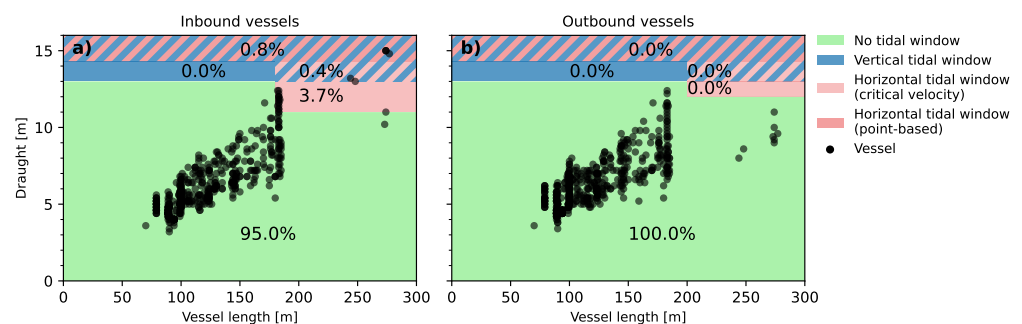


**Figure 7.** Tidal restrictions of the incoming (a) and outgoing (b) vessels, based on the vessel’s length and draught, according to Tables 1 and 2.

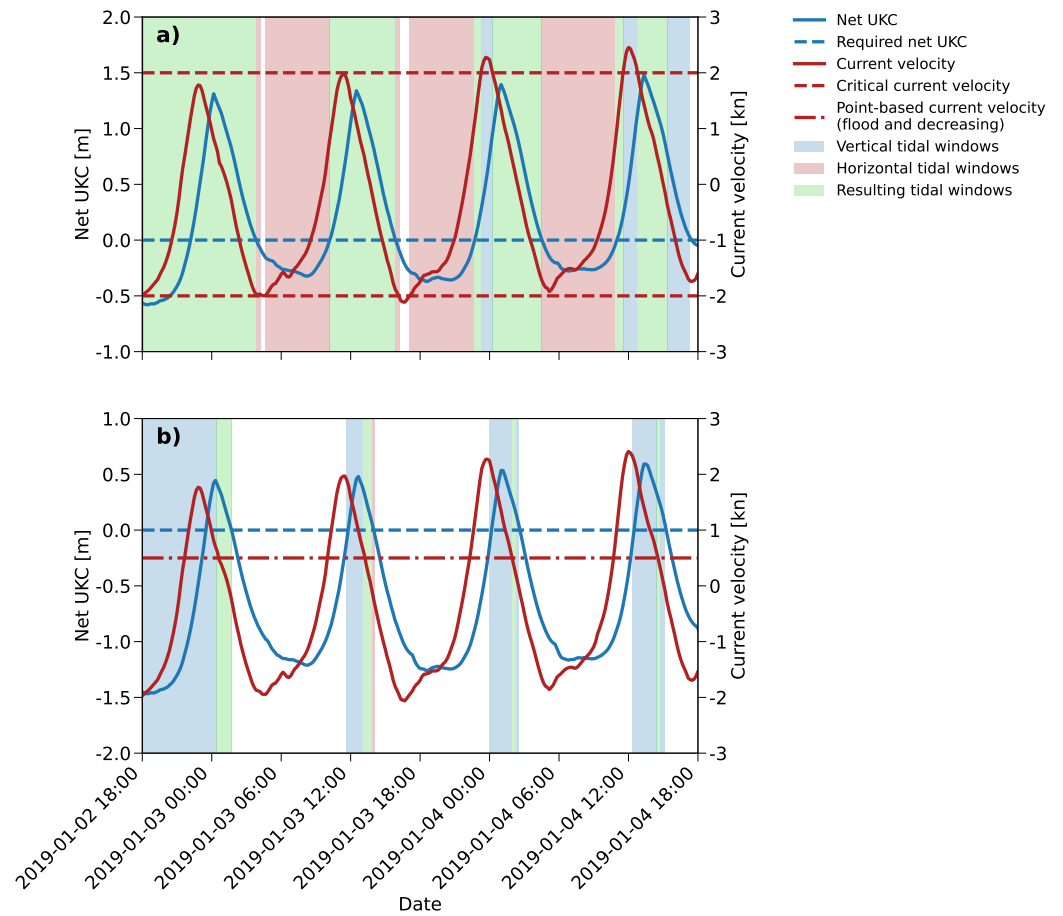


**Figure 8.** Examples of a tidal window calculations: vertical tidal windows, governed by the net UKC (left axis; a positive value means excess water depth), with horizontal tidal windows based on a critical current velocity (a), of which the absolute should be smaller and equal to 2 kn during flood (positive currents) and ebb (negative currents), and a point-based current velocity (b), which should be 0.5 kn (during flood only) with a positive and negative spreading of both 30% based on practice (right axis).

#### 4.2. Nautical Traffic Model

##### 4.2.1. Estimation of the Total Waiting Time

To align the nautical traffic model with the AIS data analysis, we simulated the 481 voyages of 255 vessels in the nautical traffic model and observed that 46.5% of the total laytimes in the anchorage areas could be resolved (see Figure 9a); 53.5% of the observed laytimes, consisting of the pink slices in this Figure (43.6% + 9.9%), were unresolved. For 60.7% of voyages, the laytimes at the anchorage area were modelled in exact accordance with the observations (less than 10 min of difference). Additionally, the model correctly estimated any form of waiting time for 18.7% of other voyages with observed laytime in the anchorage area, however, with some discrepancy. Hence, for the remaining 20.6% of voyages, the model could not resolve any of the observed laytime in the anchorage area.

For 99.0% of voyages that were modelled correctly, the vessels did not have any observed laytime in the anchorage area, which was, hence, confirmed by the model. The nautical traffic model furthermore predicted only once an exceedance of the observed laytime (no laytime was observed) by 6 min and 40 s due to waiting time for a tidal window. The remaining 1.0% of the correctly modelled voyages were made by New Panamax-class vessels that did have observed waiting time in the anchorage area.

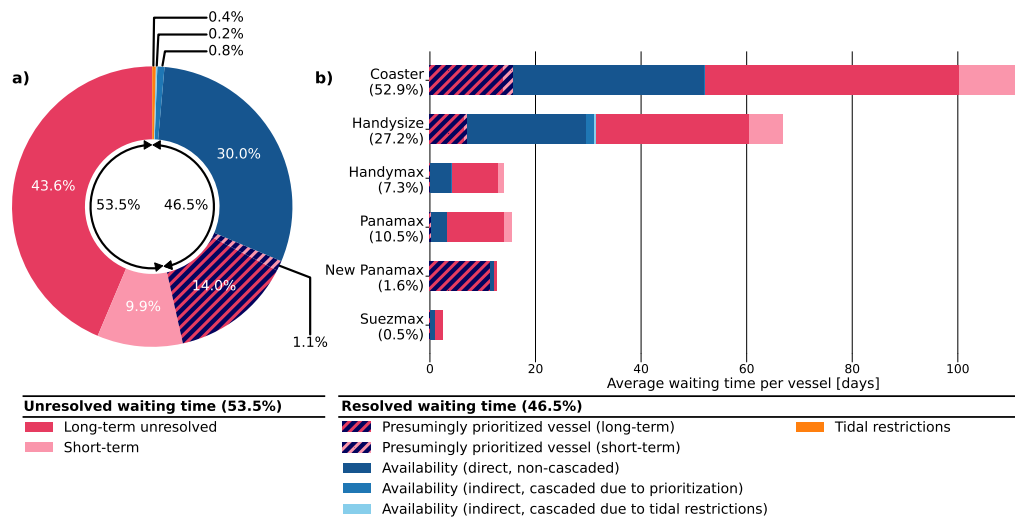


**Figure 9.** The causes of the total (a) and vessel type specific (b) laytimes of the vessels of call in the anchorage area for the base case and for the scenario without inclusion of prioritization.

#### 4.2.2. Underlying Causes for the Waiting Time

From Figure 9 we observe that congestion due to berth unavailability (30.0%) contributes most to the resolved laytimes and is partly caused by prioritization (14.0% + 1.2% + 0.8% cascading). Tidal restrictions (0.4% + 0.2% cascading) are of secondary importance for the laytimes. This is according to the expectations, as the NWW are designed for vessels with draughts up to 15.0 m, which led to only 4.9% of the vessels of the inbound trips being prone to tidal restrictions. Partly as a consequence, cascading effects contributed to 1.0% of the resolved laytimes in the anchorage area. The unavailability of the turning time did not result in additional waiting times, but this waiting time may be hidden in additional laytime of vessels at the terminal.

The model implied that 18.7% of the voyages were subject to waiting time due to terminal congestion. Most of these voyages were executed by coasters (53.5%) and Handysize-class vessels (33.3%), while the rest of the waiting time due to berth unavailability was found for voyages made by Handymax-class vessels (4.4%), Panamax-class vessels (6.7%), New Panamax-class vessels (1.1%), and Suezmax-class vessels (1.1%). This distribution is slightly shifted to the smaller vessels, compared to fleet composition (see Section 4.1). The main cause of this congestion was found to be the irregular arrival time of vessels, rather than the excessive laytimes at the terminal for some vessels, as we observed in the AIS data. These extreme laytimes of more than 2 days that caused other vessels to wait at the anchorage area only contributed to 6.2% of the total waiting time due to terminal congestion. Although the underlying causes for the excessive laytimes at the terminal are not known, the majority is expected to occur during no active call for the specific berth at which the vessel is laying (idle). Unwanted excessive laytimes may have been caused by breakdowns of terminal equipment or vessel, or spills. However, these do not occur frequently.

During 36.7% of the voyages with waiting time due to berth congestion, the vessel presumably gave priority to other vessels; during 8.5% of the total trips, a vessel moved ahead at the expense of another vessel. It is, however, debatable whether prioritization is the main reason for this waiting time. This was confirmed by experts in the field, as the vessels are in principle scheduled according to First Come First Serve (FCFS). First, only half of the time ‘priority’ was given to a larger vessel. Second, long additional waiting times of on average more than 17 h were found for which prioritizing may not pay off. Third, a considerable amount of waiting time due to prioritization was found for a New Panamax-class vessel, which waited over 11 days in the anchorage area. It was estimated that in only 1.0% of the voyages, prioritization could potentially have been a motive to wait in the anchorage area, explaining only 1.1% of the total observed laytime in the

anchorage, rather than the full 15.1%. In this case, cascading effects due to prioritization would not occur. We assume that none of the vessels gave priority in reality, and consider the resolved waiting time due to prioritization as unresolved waiting time. An additional run without prioritization shows that the resolved laytime of vessels in the anchorage areas drops to 37.3%.

Only 1.2% of the total voyages were predicted by the model to have a waiting time due to the tidal restrictions, leading to very little waiting time in the anchorage area. The horizontal tidal restrictions were found to be governing; 50.0% of the vessels that had to wait for these restrictions were limited by a critical tidal current velocity, while the other 50.0% vessels experienced waiting time due to the strict point-based tidal window, with a maximum of 9 h and 41 min. Since this contributed to 9.7% of the total turnaround time of this specific vessel, tidal accessibility remains important at vessel level. Since two of the four vessels, which were prone to a strict tidal window of only 20 min per tide, did not have to wait more than an hour, we expect that most of the waiting time in the anchorage area due to tidal windows is prevented due to careful prior planning in which vessels adjust their sailing speed at sea to arrive at the port during a tidal window.

Cascading effects were mainly triggered by vessels that presumably let other vessels go ahead (prioritization). Also, the waiting times due to tidal restrictions caused additional waiting times for non-tide-bound vessels.

#### 4.2.3. Discrepancies with the Observed Waiting Time

Accounting for only congestion (30.0%) and tidal windows (0.4% + 0.2% cascaded), 69.6% of the total observed laytimes in the anchorage area could not be resolved by the model. The observed discrepancies can be subdivided into long-term (43.6% + 14.0%) and short-term (9.9% + 1.1%) unresolved waiting times, and loading and unloading vessels (see Figure 10). These categories are discussed below based on feedback from experts of the PoR.

In Figure 10, we see that most unresolved waiting time is for loading vessels (75.8%) of which 61.1% is long-term with an average waiting time of around 16 h. 94.0% of the long-term waiting vessels are coasters (54.5%), Handysize class (33.4%), and Handymax class (6.1%) vessels (see Figure 10b). We observe a wide distribution of waiting times up to long waiting times for vessels that are to be loaded. These long, excessive laytimes are expected to be mainly caused by (a combination of) contractual obligations, and availability of the cargo/facilities at the terminal. For vessels that are hired by a party to load new cargo, sailing to the port as early as possible may be part of contractual obligations. These vessels arrive at the port and wait for the actual order to be fulfilled. Furthermore, since the terminal is processing the liquid bulk products, it may occasionally occur that the cargo is not yet ready to be shipped. Moreover, cargo may be lacking as the terminal is awaiting an import transshipment of another vessel. Since we could deduce that the liquid bulk terminal is an import terminal, mainly smaller vessels are expected to be subject to these forms of waiting time. The shorter-term unresolved laytimes for loading vessels, which contribute to 38.9% of the total (see Figure 10), can also be explained by the above-mentioned processes. This form of waiting time is also dominated by the smaller vessel classes (95.2%). Like the long-term unresolved waiting time, this is because bigger class vessels constitute only 3.3% of the loading vessels. Relatively, these latter vessels contribute most to the long-term unresolved waiting time, while the short-term contribution is more or less equal to vessels of smaller vessel classes.

On the other hand, we observe in Figure 10 that only 24.2% of the unresolved laytime is found for unloading vessels, of which 40.0% was found to be long-term. 27.8% of this long-term unresolved laytime belongs to the Panamax class (16.6%), New Panamax class (5.6%), and Suezmax class (5.6%) vessels. These long-term unresolved laytimes may be related to price speculations and negotiations. Especially the larger, loaded (to be unloaded) liquid bulk carriers may want to anchor for an additional time as the market price for the transhipped cargo may rise. Next to these speculations, negotiations about the final

price may not have been terminated before the arrival of the vessel. An example may be the Suezmax class vessel, which waited for an extra day and a half. In addition to the readiness of the cargo, the larger vessels may be prone to the unavailability of facilities at the terminal, such as the storage tanks. The long wait of 11 days for the New Panamax-class vessel may have been related to the above reasons (see Figure 9). Smaller unloading vessels, contributing to 72.2% of the long-term unresolved waiting time, are also prone to these waiting times. However, most unresolved waiting times for the unloading vessels of smaller classes are generally short-term and are more pronounced than the long-term waiting times. For the larger vessel classes, the unresolved waiting times are more or less equally divided between short- and long-term.

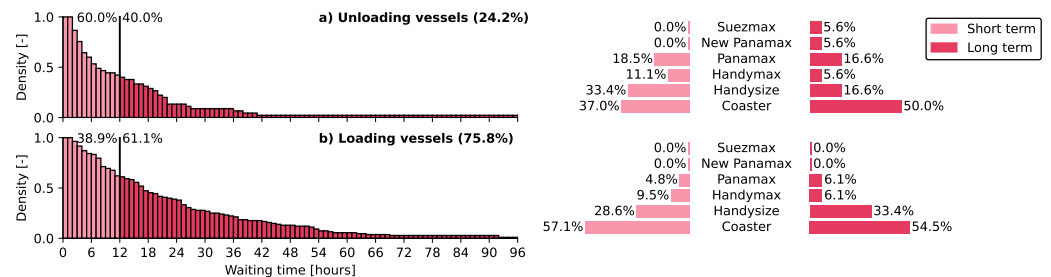


**Figure 10.** Inverse cumulative distributions of the discrepancies of unloading (a) and loading (b) vessels, including the number of vessels that had unresolved waiting times.

The (long-term) discrepancies can also be composed of a combination of frequent short-term disruptions. First, based on interviews with captains of tanker vessels, performed by Römers [63], delays due to poor communication and coordination with the shore may cause small waiting times for vessels in the anchorage. For example, updates on berth availability are rarely provided to these waiting vessels. This causes additional waiting times that are not resolved with the model, as the communication in this model is assumed to be optimal. 40.0% of the vessels that would be loading at the terminal had a short-term unresolved waiting time of less than 4 h, while having resolved waiting time due to berth congestion (see Figure 10a).

Second, congestion due to the limited availability of tugs and pilots occurs frequently in the PoR. This waiting time will typically not last longer than 2 h and waiting for towage is reported to be the most frequent cause for waiting time [39]. During busy periods and extremely windy conditions, the increased demand for tugs and pilots may even cause waiting times of 3 to 4 h. It is questionable whether this effect is major for this particular terminal, as most vessels with unresolved laytimes do not require tug assistance (classes smaller than Handymax class). Waiting for pilotage, however, could contribute to the waiting times of the other types of vessels; in total 10 Panamax-class vessels had short-term unresolved waiting times (see Figure 10). Another potential reason for the short-term discrepancy in waiting times is due to congestion of the waterway.

Third, vessels could have potentially waited during the downtime of the port due to other consequences than tidal restrictions, such as fog, wind, or storms. The importance of this downtime is debatable as its occurrence is infrequent. Other downtimes may theoretically be caused by daylight and working hours of the terminal, but this is not influential for this terminal; departures and arrivals occur almost uniformly over the full period of the day. Less frequent reasons for the long-term discrepancies may be the unavailability of berths due to barges, special operations, and calamities. It is, however, believed that sea-going vessels do have priority over barges. Special operations such as lightening operations of large vessels that are otherwise not able to enter the port directly due to draught restrictions, are not applicable for the PoR. Calamities of vessels that are broken down, and required reparations could have potentially caused additional waiting times, but this is very unlikely.

#### 4.2.4. Testing Alternative Maintained Bed Level Designs

We saw that terminal congestion explains most of the waiting time of the fleet, while tidal windows are less important for the fleet. This is in accordance with the port policy that states that 99.0% of the tides should be accessible for any inbound vessel with a draught of 15.0 m. Our model found that the current MBL design of the channel is slightly underdimensioned with a tidal accessibility of 98.4%.

Applying the validated model to the previous MBL design of the NWW (14.5 m instead of 16.2 m), we found that the four deepest-draughted vessels of 14.8 and 15.0 m of draught could not enter the 3rd PET. Furthermore, assuming that the tidal restrictions will now apply to vessels with a draught of 9.3 m (11.0 m – 1.7 m), more inbound trips (9.0% instead of 4.6%) will be prone to these rules. The total waiting time due to tidal restrictions, however, decreases from about 21.5 h to about 19.5 h. This is because most vessels fall in the lenient window-based current velocity regime. The percentage of vessels prone to the strict point-based current velocity tidal window decreased from 8.3% to 4.2% (with port accessibility for design vessels with draughts of 13.5 m of about 99%).

In case the exclusion of the four deepest-draughted vessels may be unacceptable, a more moderate reduction of 0.5 m in MBL of the Nieuwe Waterweg and Scheur could be undertaken. The model found that this will result in a degree of accessibility of 59.1% for the design vessel, leading to an increase of the total modelled waiting times of 33.6%. This increase consists of 73.4% of waiting time due to cascading effects of the tidal window; the rest (26.6%) is waiting time directly caused by the tidal restrictions. On the contrary, based on Figure 7, we see that more considerable gains in the reduction of the MBL can be obtained by redirecting the deepest-draughted New Panamax and Suezmax class vessels to other deep-sea terminals (i.e., Maasvlakte). The model found that by diverting the 9 deepest-drafted vessels, the desired service level could be achieved with MBLs that are 3.0 m higher than the current MBLs. More vessels will then be prone to a tidal window, but the increase in the total waiting time will only be 2.7%, while dredging costs are potentially lower.

## 5. Discussion

### 5.1. Interpretation of the Results

Based on our quantification of the vessels' waiting times at a liquid bulk terminal in the PoR, we found that the terminal operates efficiently. Depending on the actual causes of the unresolved waiting time, and the presumed prioritization in particular, congestion should be further limited to improve the terminal's efficiency. As the terminal area is scarce, optimization of land-based and berth planning and occupancy may have to be considered. A more in-depth study of the actual causes of the waiting time is therefore recommended. For the port authority, this can discover bottlenecks due to limitations in port infrastructure, or whether waiting time can be accepted.

Regarding the MBL design and policy of tidal restrictions that are set by the port authority, the results show a high degree of accessibility to the liquid bulk terminal. For the deepest-draughted design vessel, the port accessibility is sufficient. It can be further improved by investigating the point-based horizontal tidal restriction which is the main limiting factor. A further deepening of the NWW, based on the current design vessel, is not required. On the contrary, our work shows that a less deep NWW is not recommended either, as this results in significant waiting times for the design vessel and cascading waiting times for other vessels of call.

From a fleet perspective, however, the waiting times due to the tidal restrictions are limited. Since only 0.6% of the vessels require the MBL design of the NWW, a significant reduction in the dredging requirements can be accomplished by diverting the deepest-draughted vessels to more offshore-located terminals. A further study considering more inland terminals can quantify the feasibility and effects of such an intervention. Special attention should be given to the attractiveness of the port. Shipowners and shipping companies may not be retained by the PoR when subjected to tidal restrictions or diversions

to other terminals [64,65]. The performance of the nautical traffic model in different scenarios should be tested further, for example by simulating the situation during the shallower NWW before 2019.

### 5.2. Further Challenges to Overcome the Approach's Limitations

Although the results on the quantification of the waiting times are promising, we still found significant discrepancies between the modelled and observed laytimes of vessels in the anchorage area. The method has several limitations that may have to be addressed in future studies.

First, the model presented here relies on an extensive set of geospatial, hydrodynamic, and AIS data. In other case studies, these datasets may be unavailable. The availability of hydrodynamic data, for instance, depends on measurement campaigns and/or numerical models, which may be lacking and are costly to set up. Moreover, AIS data may be protected or absent (i.e., for new ports or future scenarios). While the availability of these datasets is expected to improve the results significantly, the simulation model can also be used with synthetic data. Further research has to confirm this.

Second, although the processing and analysis of AIS data successfully resulted in the required information, the dependency of the model on AIS is not fully reliable and could have potentially led to errors in the set up and validation of the hindcast simulation with the nautical traffic model. AIS data are known to contain errors in the manual, static (i.e., draught) and dynamic (i.e., Global Positioning System (GPS), SOG) information, which was also observed in this research. As severe GPS errors caused idle vessels to drift in space, our method could occasionally not distinguish idle from sailing vessels. These errors have potentially resulted in erroneous laytimes of vessels at the wrong infrastructure. Contributing to this problem was the fact that AIS data were sometimes lacking around the berth areas, seemingly caused by the operators of the vessel that forgot to switch on the AIS. We limited these errors by removing outliers based on the SOG, but this parameter was found to include inadequacies as well. The outlier removal process could therefore not be fully relied upon, and some errors remained to be present. A more extensive analysis should be investigated, as it may be required for further studies.

Third, various port processes have been neglected in this model that may explain part of the discrepancies and/or may be required in different case studies but were deemed out of scope in this research. Most prominently, the land-based terminal operations were disregarded [18,66]. These are thought to cause significant long-term, cascading waiting times for vessels of several hours to days. Based on expert judgement, cargo is occasionally not ready for (un)loading. This is, for example, caused by delayed preceding vessels or delays in the processing of cargo at the terminal. We therefore strongly recommend a study involving the development and validation of a fast discrete-event model to simulate terminal operations jointly with the nautical traffic.

Other omitted processes that could have resulted in resolving more short-term waiting times are waterway congestion due to ambient traffic [55], traffic regulations such as in the Rio de la Plata [41], congestion due to limited tug and pilot availability [39], and downtime due to other external environmental conditions [67]. These processes may interact with each other, as more adverse weather conditions (i.e., strong winds from particular directions) may lead to a higher demand for tugs and pilots, which can exceed their capacity during peak traffic flows. Depending on the specific case, further research on the cascading waiting times due to such processes is advised.

Other neglected processes that affect the speed of vessels, and could have led to delays in the order of several minutes, are vessel encounters and overtaking, vessel properties (i.e., draught), and meteo-hydrological conditions (i.e., currents and winds) [68]. Modelling the correct speed for tide-bound vessels is important to calculate the tidal windows. In this study, due to the short distances and few tide-bound vessels, this would not have led to different results. However, we believe that the above-mentioned processes should be included in further studies.



Fourth, some port infrastructure and traffic management processes have been neglected in this research. Apart from the land-based operations at terminals, other terminal types have not been considered, such as container and dry bulk terminals with a quay instead of jetties. While jetties have a unit capacity, quay-type terminals also have limited crane or excavator equipment that determines the laytime of vessels at the terminal. Scheduling of these cranes based on vessel demand is a port process that has to be added to the nautical traffic model in further research. This can be a fast integrated berth-allocation and quay crane-assignment problem, as presented in Çagatay et al. [69]. The same holds for the capacity of anchorage areas [70], and waterway traffic management [71]. The inclusion of jetty-allocation plans, such as Sienz and Innocente [72], in the nautical traffic model is for further research.

Last, the mapping of the AIS tracks onto the network has led to errors in vessel speed. Vessels did not necessarily follow the simplified network. This has contributed to errors in the delays in the order of several minutes. Future research may need to overcome this simplification for cases where small deviations like this are considered problematic.

### 5.3. Significance of the Method for New Applications

Although many improvements to the model are possible, we want to stress that our data-driven modelling approach already gives very promising results. By including realistic hydrodynamics, detailed accessibility policies and berth availability information, the model was able to rapidly quantify and resolve the fleet's laytime in the anchorage area due to the cascading delays of terminal congestion and tidal restrictions. Furthermore, we were able to create a relation between the degree of accessibility of ports, which for the 3rd PET was in accordance with De Jong [60], and the waiting time of vessels. Therefore, our approach is able to test alternative MBL designs based on the impact of the fleet's waiting time, rather than on the accessibility percentage of a single design vessel. This is a significant advantage over design-vessel approaches. In particular, the quantification of the cascading effects proved to be highly important for this. Although these effects have a limited effect on the fleet's waiting time in the current situation, we observed that they become increasingly important when the MBL become shallower and more vessels are affected by the tidal restrictions.

We would also like to mention that the open-source environment of the nautical traffic model enables an excellent opportunity to include further improvements to the model, in joint development with other researchers and stakeholders. We expect that the model is capable of incorporating omitted port processes and infrastructure with minor additions and alterations. Besides, the model is not limited to the hindcast study that was presented in this paper. We anticipate that the model can be implemented in worldwide port and waterway systems for various other purposes. The model could namely be used as an operational tool for real-time modelling or nowcasting to, for example, optimize short-term planning of operations. Moreover, the model can be applied as a forecasting tool on tactical (medium-term) and strategic (long-term) levels, namely to test alternative traffic regulations, accessibility policies, vessel-priority rules, waterway and berth layouts, and the effect of changing fleets of call on the port. Probabilistic and machine-learning tools on AIS data are required to assist in these model applications. Most distinctively, the model is also suitable for integral design in areas with multiple stakeholders, as it is coupled with a hydrodynamic model. This is particularly useful when modelling alternative port infrastructure designs and port expansions, which may alter the hydrodynamics (i.e., channel deepening, and construction of new harbour basins). Such interventions may lead to enhanced salt intrusion and additional sedimentation and turbidity (see [1]), which are important for the functioning of ports and the local society. We foresee further research on such integral topics, as they are becoming more and more important.

## 6. Conclusions

The work in this paper was triggered by the observation that port accessibility designs are typically based on design vessels while neglecting or simplifying important, cascading waiting times for a representative fleet of vessels due to congestion and port downtime. Such strategies may lead to sub-optimal port and waterway designs.

To investigate this, a method was envisioned that simultaneously accounts for (1) realistic hydrodynamics, (2) detailed accessibility policies, (3) realistic vessel properties, (4) cascading effects of vessel-priority rules, (5) detailed waterway and berth layout, and (6) concrete berth-allocation policies. It was postulated that such a method does not as yet exist. Therefore, we developed a discrete-event model that simulates nautical traffic by including these aspects of tidal downtime and infrastructure congestion. The model requires a geospatial graph of the port network, resources that schematise the port infrastructure (i.e., terminals, anchorage areas, and turning basins), agents with properties that represent the vessels of call (i.e., arrival times, draughts, laytimes at the terminal and turning basins), and tidal and traffic restrictions, including vessel speeds and realistic hydrodynamics over the graph. We applied the simulation model to a real-world case study of a liquid bulk terminal in the 3rd PET of the PoR. To derive the required information for this model, we jointly analysed geospatial data, AIS data, and hydrodynamic data from a numerical model. The approach was designed to result in a detailed decomposition of the causes of the fleet's waiting time, which were validated against the observations in AIS data.

Using the mentioned data sources, we could successfully deploy the nautical traffic model, leading to a reproduction of 73.4% of the non-excessive laytimes, modelling 60.7% of the vessels-of-call in accordance with the observations. 98.0% of the observed waiting time was resolved by the model as terminal congestion while waiting time due to tidal restrictions was limited to only 2.0% of the observed waiting time. This finding met our expectations, as the channel's MBL is designed for the deepest draughted design vessel that comprises 0.6% of the fleet. Consequently, only 5.0% of the fleet was prone to tidal restrictions, with 1.2% of the fleet having consequential waiting times. The resolved waiting time that was allegedly caused by vessel priority rules was excluded, as experts confirmed that such rules are not in place. Therefore, the cascading effects of tidal restrictions and vessel priority rules were limited for this specific case study. However, by running various alternative MBL designs, these cascading effects became important, highlighting the added value of the modelling approach of a fleet over a design vessel approach.

Still, a discrepancy of 69.2% between the modelled and observed laytimes was found. Most of this waiting time is expected not to be related to the wet infrastructure, but due to (cascading) congestion in cargo flows and other economic considerations. For further studies, improvements to the model may therefore be required. The open-source, and modular structure of the nautical traffic model is highly suitable for this. Despite these potential improvements, the model's current performance is satisfactory. We have high confidence that our modelling approach will eventually enable us to analyse the inefficiency of the total port system while uncovering the specific, underlying contribution of each specific component. In this way, we can make rational improvements to the port's wet infrastructure.

**Author Contributions:** Conceptualization, F.P.B., S.v.d.W., F.B., A.K., S.d.J. and M.v.K.; methodology, F.P.B.; software, F.P.B., S.v.d.W., F.B. and M.v.K.; validation, F.P.B.; formal analysis, F.P.B.; investigation, F.P.B.; resources, F.P.B. and S.v.d.W.; data curation, F.B.; writing—original draft preparation, F.P.B.; writing—review and editing, S.d.J., F.B., A.K., S.v.d.W. and M.v.K.; visualization, F.P.B.; supervision, M.v.K.; project administration, M.v.K.; funding acquisition, M.v.K. All authors have read and agreed to the published version of the manuscript.

**Funding:** The work for this publication is part of SALTISolutions, which is a Perspective Programme (partly) funded by the Dutch Research Council (NWO). More specifically the work presented here is part of P18-32 Project 7 "Design and operation of nature-based SALTISolutions".

**Institutional Review Board Statement:** Not applicable.

**Informed Consent Statement:** Not applicable.

**Data Availability Statement:** The original data presented in the study are reproducible using Bakker et al. [61]. Restrictions apply to the availability of the raw data. Data were obtained from Rijkswaterstaat and the Port of Rotterdam.

**Acknowledgments:** We would like to express our gratitude to the Port of Rotterdam which provided part of the geospatial data and, in particular, Lamber Hulsen, who provided the hydrodynamic data. Furthermore, we would like to thank Rijkswaterstaat for providing the AIS data and the FIS graph.

**Conflicts of Interest:** Fedor Baart was partly employed by Deltares, and Mark van Koningsveld was partly employed by Van Oord Dredging and Marine Contractors BV. The remaining authors declare that the research was conducted in the absence of any commercial or financial relationships that could be construed as a potential conflict of interest.

## Abbreviations

The following abbreviations are used in this manuscript:

3rd PET	3rd Petroleumhaven
AIS	Automatic Identification System
GPS	Global Positioning System
FIS	Fairway Information System
FWA	Fresh Water Allowance
pdf	Probability Density Function
MBL	Maintained Bed Level
NWW	New Waterway
PoR	Port of Rotterdam
SOG	Speed Over Ground
TSS	Traffic Separation Scheme
UKC	Under Keel Clearance

## References

- Siemes, R.; Duong, T.M.; Willemsen, P.; Borsje, B.; Hulscher, S. Morphological Response of a Highly Engineered Estuary to Altering Channel Depth and Restoring Wetlands. *J. Mar. Sci. Eng.* **2023**, *11*, 2150. [\[CrossRef\]](#)
- Van Koningsveld, M.; Verheij, H.; Taneja, P.; De Vriend, H. *Ports and Waterways: Navigating the Changing World*; TU Delft Open: Delft, The Netherlands, 2023.
- Bakker, F.P.; Van Koningsveld, M. Optimizing bed levels in ports based on port accessibility. In Proceedings of the International Conference on Coastal Engineering (ICCE), Sydney, Australia, 4–9 December 2022; Volume 37, p. 11. [\[CrossRef\]](#)
- PIANC. *Harbour Approach Channels—Design Guidelines*; Technical Report; Permanent International Commission for Navigation Congresses (PIANC): Brussels, Belgium, 2014.
- Bos, M.; Koop, O.; Bolt, E. Safety Level of a Probabilistic Admittance Policy. In Proceedings of the ASME 2011 30th International Conference on Ocean, Offshore and Arctic Engineering OMAE, Rotterdam, The Netherlands, 19–24 June 2011; pp. 263–271. [\[CrossRef\]](#)
- Vantorre, M.; Candries, M.; Verwilligen, J. Optimization of Tidal Windows for Deep-Drafted Vessels by Means of ProToel. In Proceedings of the International Workshop on Next Generation Nautical Traffic Models, Delft, The Netherlands, 5–7 June 2013.
- Masalaci, B.; Zorba, Y. An application of agent-based traffic flow model for maritime management evaluation. *Int. J. Marit. Eng.* **2023**, *165*, 55–69. [\[CrossRef\]](#)
- De Alvarenga Rosa, R.; Ribeiro, G.M.; Mauri, G.R.; Fracaroli, W. Planning the berth allocation problem in developing countries with multiple cargos and cargo priority by a mathematical model and a clustering search metaheuristic. *Int. J. Logist. Syst. Manag.* **2017**, *28*, 397–418. [\[CrossRef\]](#)
- Venturini, G.; Iris, Ç.; Kontovas, C.A.; Larsen, A. The multi-port berth allocation problem with speed optimization and emission considerations. *Transp. Res. Part D Transp. Environ.* **2017**, *54*, 142–159. [\[CrossRef\]](#)
- Kramer, A.; Lalla-Ruiz, E.; Iori, M.; Voß, S. Novel formulations and modeling enhancements for the dynamic berth allocation problem. *Eur. J. Oper. Res.* **2019**, *278*, 170–185. [\[CrossRef\]](#)
- Jia, S.; Li, C.L.; Xu, Z. Managing navigation channel traffic and anchorage area utilization of a container port. *Transp. Sci.* **2019**, *53*, 728–745. [\[CrossRef\]](#)
- Zhang, B.; Zheng, Z.; Wang, D. A model and algorithm for vessel scheduling through a two-way tidal channel. *Marit. Policy Manag.* **2020**, *47*, 188–202. [\[CrossRef\]](#)

13. Xiao, F.; Ligteringen, H.; Van Gulijk, C.; Ale, B. Nautical traffic simulation with multi-agent system. In Proceedings of the 16th International IEEE Annual Conference on Intelligent Transportation Systems, ITSC, The Hague, The Netherlands, 6–9 October 2013; pp. 1245–1252.
14. Bellsolà Olba, X.; Daamen, W.; Vellinga, T.; Hoogendoorn, S.P. Estimating Port Network Traffic Capacity. *Sci. J. Marit. Univ. Szczec.* **2015**, *42*, 45–53. [[CrossRef](#)] [[PubMed](#)]
15. Shu, Y.; Daamen, W.; Ligteringen, H.; Hoogendoorn, S. Operational model for vessel traffic using optimal control and calibration. *Sci. J. Marit. Univ. Szczec.* **2015**, *42*, 70–77.
16. Xin, X.; Liu, K.; Yang, X.; Yuan, Z.; Zhang, J. A simulation model for ship navigation in the “Xiazhimen” waterway based on statistical analysis of AIS data. *Ocean. Eng.* **2019**, *180*, 279–289. [[CrossRef](#)]
17. Durlík, I.; Gucma, L.; Miller, T. applied sciences Statistical Model of Ship Delays on the Fairway in Terms of Restrictions Resulting from the Port Regulations: Case Study of Swinoujscie-Szczecin Fairway. *Appl. Sci.* **2023**, *13*, 5271. [[CrossRef](#)]
18. Carteni, A.; Luca, S.D. Tactical and strategic planning for a container terminal: Modelling issues within a discrete event simulation approach. *Simul. Model. Pract. Theory* **2012**, *21*, 123–145. [[CrossRef](#)]
19. Iannone, R.; Miranda, S.; Prisco, L.; Riemma, S.; Sarno, D. Proposal for a flexible discrete event simulation model for assessing the daily operation decisions in a Ro-Ro terminal. *Simul. Model. Pract. Theory* **2016**, *61*, 28–46. [[CrossRef](#)]
20. Wahed, M.A.; Faghri, A.; Li, M. An innovative simulation model for the operations of a multipurpose seaport: A case study from Port of Wilmington, USA. *Int. J. Simul. Process. Model.* **2017**, *12*, 151–164. [[CrossRef](#)]
21. Leal, L.R. Stochastic Simulation of an Oil Terminal To Reduce the Turnaround Time of Tankers Through Pipeline Operability. In Proceedings of the Brazilian Symposium on Operations Research, Rio de Janeiro, Brazil, 6–9 August 2018.
22. Neagoe, M.; Hvolby, H.H.; Taskhiri, M.S.; Turner, P. Using discrete-event simulation to compare congestion management initiatives at a port terminal. *Simul. Model. Pract. Theory* **2021**, *112*, 102362. [[CrossRef](#)]
23. Koldborg Jensen, T.; Gamborg Hansen, M.; Lehn-Schiøler, T.; Melchild, K.; Mølsted Rasmussen, F.; Ennemark, F. Free flow efficiency of a one-way traffic lane between two pylons. *J. Navig.* **2013**, *66*, 941–951. [[CrossRef](#)]
24. Tassedda, E.H.; Shoji, R. Statistical Modeling Framework of Vessel Traffic Streams in Tokyo Bay. *Trans. Navig.* **2018**, *3*, 31–42.
25. Dragovic, B.; Zrníc, N.; Twrdy, E. Ship Traffic Modeling and Performance Evaluation in Container Port. *Analele Univ. “Eftimie Murgu” Reșița* **2012**, *XVII*, 127–138.
26. Navarro, M.; Bano, R.; Cheng, M.; Torres, M.; Kurata, Y.B.; Gutierrez, T. Queuing Theory Application using Model Simulation: Solution to address Manila Port congestion. In Proceedings of the Asia Pacific Industrial Engineering & Management Systems Conference, Ho Chi Minh City, Vietnam, 8–11 December 2015; pp. 1109–1114.
27. Hansen, J.B. Optimizing Ports through Computer Simulation Sensitivity Analysis of Pertinent Parameters. *Oper. Res. Q.* **1972**, *23*, 519–530. [[CrossRef](#)]
28. Park, C.S.; Noh, Y.D. An interactive port capacity expansion simulation model. *Eng. Costs Prod. Econ.* **1987**, *11*, 109–124. [[CrossRef](#)]
29. Kondratowicz, L.J. Methodological solutions for increased efficiency of modelling and simulation of seaports and inland freight terminals. *Marit. Policy Manag.* **1992**, *19*, 157–164. [[CrossRef](#)]
30. Hassan, S.A. Port activity simulation: An overview. *ACM SIGSIM Simul. Dig.* **1993**, *23*, 17–36. [[CrossRef](#)]
31. Demirci, E. Simulation Modelling and Analysis of a Port Investment. *Simulation* **2003**, *79*, 94–105. [[CrossRef](#)]
32. Howard, D.L.; Bragen, M.J.; Burke, J.F.; Love, R.J. PORTSIM5: Modelling from a Seaport Level. *Math. Comput. Model.* **2004**, *39*, 715–731. [[CrossRef](#)]
33. Arango, C.; Cortés, P.; Muñuzuri, J.; Onieva, L. Berth allocation planning in Seville inland port by simulation and optimisation. *Adv. Eng. Inform.* **2011**, *25*, 452–461. [[CrossRef](#)]
34. Ugurlu, Ö.; Yükksey, E. Simulation Model on Determining of Port Capacity and Queue Size: A Case Study for BOTAS Ceyhan Marine Terminal. *Int. J. Mar. Navig. Safety Sea Transp.* **2014**, *8*, 143–150. [[CrossRef](#)]
35. Clark, T.; Kabil, M.; Moussa Mostafa, M. An analysis and simulation of an experimental suez canal traffic control system. In Proceedings of the 1983 Winter Simulation Conference, Arlington, VA, USA, 12–14 December 1983; pp. 311–318.
36. Van de Ruit, G.; Van Schuylenburg, M.; Ottjes, J. Simulation of shipping traffic flow in the Maasvlakte port area. In Proceedings of the European Simulation Multiconference (ESM), Prague, Czech Republic, 5–7 June 1995.
37. Yeo, G.T.; Roe, M.; Soak, S.M. Evaluation of the Marine Traffic Congestion of North Harbor in Busan Port. *J. Waterw. Port Coast. Ocean. Eng.* **2007**, *133*, 87–93. [[CrossRef](#)]
38. Fransen, R.; Tilanus, P.; de Jong, J.; Davydenko, I. *Swarmport Agent-Based Simulation Model Description and Documentation*; Technical Report; TNO: The Hague, The Netherlands, 2021.
39. Nikghadam, S. Cooperation between Vessel Service Providers for Port Call Performance Improvement. Ph.D. Thesis, Delft University of Technology, Delft, The Netherlands, 2023. [[CrossRef](#)]
40. Groenveld, R. *HARBORSIM: A Generally Applicable Harbour Simulation Model*; Technical Report; Delft University of Technology, Department of Civil Engineering, Hydraulig Engineering Group: Delft, The Netherlands, 1983.
41. Frima, G. Capacity Study for the Rio de la Plata Waterway, Argentina. Master’s Thesis, Delft University of Technology, Delft, The Netherlands, 2004.
42. Moser, D.; Hofseth, K.; Heisey, S.; Males, R.; Rogers, C. *HARBORSYM: A Data-Driven Monte Carlo Simulation Model of Vessel Movement in Harbors*; Technical Report; Institute for Water Resources U.S. Army Corps of Engineers: Alexandria, VA, USA, 2004.

43. Macquart, A. Simulation Model to Assess the Effective Capacity of the Wet Infrastructure of a Port. Master's Thesis, Delft University of Technology, Delft, The Netherlands, 2007.
44. Rayo, S. Development of a Simulation Model for the Assessment of Approach Channels—The Tasman Seaport Case. Master's Thesis, Delft University of Technology, Delft, The Netherlands, 2013.
45. Piccoli, C. Assessment of Port Marine Operations Performance by Means of Simulation. Case Study: The Port of Jebel Dhanna/Ruwais-UAE. Master's Thesis, Delft University of Technology, Delft, The Netherlands, 2014.
46. Tang, G.; Wang, W.; Song, X.; Guo, Z.; Yu, X.; Qiao, F. Effect of entrance channel dimensions on berth occupancy of container terminals. *Ocean. Eng.* **2016**, *117*, 174–187. [[CrossRef](#)]
47. Thiers, G.; Janssens, G. A Port Simulation Model as a Permanent Decision Instrument. *Simulation* **1998**, *71*, 117–125. [[CrossRef](#)]
48. Almaz, O.A.; Altiok, T. Simulation modeling of the vessel traffic in Delaware River: Impact of deepening on port performance. *Simul. Model. Pract. Theory* **2012**, *22*, 146–165. [[CrossRef](#)]
49. Scott, D.; Taylor, D.; El-solh, S.; Elliott, T. Port Simulation Modelling and Economic Assessment. *J. Mar. Sci. Eng.* **2016**, *4*, 16. [[CrossRef](#)]
50. Curtis, B. An Integrated Approach to Port Planning, Operations & Risk Management through Technology. In Proceedings of the PIANC-World Congress, Panama City, Panama, 7–12 May 2018.
51. Ayuso, C.; Redondo, R.; Atenza, R.; Ramón, J. Paper CA1201—SIFLOW21. Simulación predictiva de capacidad basado en análisis de datos AIS. In Proceedings of the XII Congreso Argentino de Ingeniería Portuaria, Buenos Aires, Argentina, 5–8 September 2022.
52. Franzkeit, J.; Pache, H.; Jahn, C. Investigation of Vessel Waiting Times. In Proceedings of the Dynamics in Logistics and the 7th International Conference LDIC 2020, Bremen, Germany, 12–14 February 2020; pp. 70–78. [[CrossRef](#)]
53. Ma, J.; Zhou, Y.; Zhu, Z. Identification and analysis of ship waiting behavior outside the port based on AIS data. *Sci. Rep.* **2023**, *13*, 11267. [[CrossRef](#)] [[PubMed](#)]
54. Martinicic, T.; Stepec, D.; Costa, J.P.; Cagran, K.; Chaldeakis, A. Vessel and Port Efficiency Metrics through Validated AIS data. In Proceedings of the Global Oceans, Singapore—U.S. Gulf Coast, Biloxi, MS, USA, 5–30 October 2020. [[CrossRef](#)]
55. Jafari Kang, M.; Zohoori, S.; Hamidi, M.; Wu, X. Study of narrow waterways congestion based on automatic identification system (AIS) data: A case study of Houston Ship Channel. *J. Ocean. Eng. Sci.* **2022**, *7*, 578–595. [[CrossRef](#)]
56. Steenari, J.; Lwakatare, L.; Nurminen, J.; Tolonen, J.; Manderbacka, T. Mining port operation information from AIS Data. In Proceedings of the Hamburg International Conference of Logistics (HICL), Hamburg, Germany, 21–23 September 2022; Volume 33, pp. 657–678. [[CrossRef](#)]
57. Van der Werff, S.; Baart, F.; Van Koningsveld, M. Vessel Behaviour under Varying Environmental Conditions in Coastal Areas. In Proceedings of the 35th PIANC World Congress, Cape Town, South Africa, 29 April–3 May 2024.
58. Van Koningsveld, M.; Den Uijl, J. OpenTNSim v0.0.1, 2019. Zenodo. Available online: <https://zenodo.org/records/3341517> (accessed on 13 May 2024).
59. Baart, F.; Jiang, M.; Bakker, F.P.; Frijlink, T.; Van Koningsveld, M. OpenTNSim v1.2.0, 2022. Zenodo. Available online: <https://zenodo.org/records/7053274> (accessed on 13 May 2024).
60. De Jong, S. Assessing Maintained Bed Levels in ports. Master's Thesis, Delft University of Technology, Delft, The Netherlands, 2020.
61. Bakker, F.; Baart, F.; Van Koningsveld, M. OpenTNSim-v1.4.0-paper.3, 2024. Zenodo. Available online: <https://zenodo.org/records/11489436> (accessed on 13 May 2024).
62. Abreu, F.H.; Soares, A.; Paulovich, F.V.; Matwin, S. A trajectory scoring tool for local anomaly detection in maritime traffic using visual analytics. *Isprs Int. J. -Geo-Inf.* **2021**, *10*, 412. [[CrossRef](#)]
63. Römers, I.E.M. Port Call Optimization in Three Oil Shipping Markets. Master's Thesis, Erasmus University Rotterdam, Rotterdam, The Netherlands, 2013.
64. Xiao, G.; Wang, T.; Shang, W.; Shu, Y.; Biancardo, S.A.; Jiang, Z. Exploring the factors affecting the performance of shipping companies based on a panel data model: A perspective of antitrust exemption and shipping alliances. *Ocean. Coast. Manag.* **2024**, *253*, 107162. [[CrossRef](#)]
65. Richmond, L.; Casali, L. The role of social capital in fishing community sustainability: Spiraling down and up in a rural California ports. *Mar. Policy* **2022**, *137*, 104934. [[CrossRef](#)]
66. Roy, D.; Scheinhart, W.; van Ommeren, J.-K. A Fluid Flow Queuing Network Model for Performance Analysis of Bulk Liquid Terminals. In Proceedings of the 16th International Material Handling Research Colloquium (IMHRC), Dresden, Germany, 19–23 July 2023.
67. Camus, P.; Tomás, A.; Díaz-Hernández, G.; Rodríguez, B.; Izaguirre, C.; Losada, I. Probabilistic assessment of port operation downtimes under climate change. *Coast. Eng.* **2021**, *154*, 12–24. [[CrossRef](#)]
68. Shu, Y.; Daamen, W.; Ligteringen, H.; Hoogendorp, S.P. Influence of external conditions and vessel encounters on vessel behavior in ports and waterways using Automatic Identification System data. *Ocean. Eng.* **2017**, *131*, 1–14. [[CrossRef](#)]
69. Çagatay, I.; Pacino, D.; Ropke, S.; Larsen, A. Integrated Berth Allocation and Quay Crane Assignment Problem: Set partitioning models and computational results. *Transp. Res. Part E Logist. Transp. Rev.* **2015**, *10*, 75–97. [[CrossRef](#)]
70. Zhao, J.; Chunhui, Z.; Li, Z.; Xu, Y.; Gan, L. Optimization of anchor position allocation considering efficiency and safety demand. *Ocean. Coast. Manag.* **2023**, *241*, 106644. [[CrossRef](#)]

71. Liu, B.; Li, Z.C.; Wang, Y.; Dian, S. Short-term berth planning and ship scheduling for a busy seaport with channel restrictions. *Transp. Res. Part E* **2021**, *154*, 102467. [[CrossRef](#)]
72. Sienz, J.; Innocente, M. *Particle Swarm Optimization: Fundamental Study and Its Application to Optimization and to Jetty Scheduling Problems*; Saxe-Coburg Publications: Stirlingshire, UK, 2008. [[CrossRef](#)]

**Disclaimer/Publisher's Note:** The statements, opinions and data contained in all publications are solely those of the individual author(s) and contributor(s) and not of MDPI and/or the editor(s). MDPI and/or the editor(s) disclaim responsibility for any injury to people or property resulting from any ideas, methods, instructions or products referred to in the content.